

## Article

# Simulation of Land Use Change and Habitat Quality in the Yellow River Basin under Multiple Scenarios

Chun Fu <sup>1</sup>, Yezhong Liu <sup>1,\*</sup>, Yudi Chen <sup>1</sup>, Fan Li <sup>1</sup>, Jinyan Huang <sup>2</sup> and Huimin Huang <sup>1</sup><sup>1</sup> School of Infrastructure Engineering, Nanchang University, Nanchang 330031, China<sup>2</sup> School of Resources & Environment, Nanchang University, Nanchang 330031, China

\* Correspondence: yezhongliu@foxmail.com

**Abstract:** Habitat quality is the key to regional ecological restoration and green development, and land use change is an essential factor affecting habitat quality. Studying the spatial and temporal evolution characteristics of land use change and habitat quality under multiple scenarios is significant for regional ecological restoration and management, and for preventing future ecological and environmental risks. We used the improved Logistic-CA-Markov (Logistic-Cellular Automata-Markov) and InVEST (Integrated Valuation of Ecosystem Services and Trade-offs) models to establish the spatial patterns of habitat quality in the Yellow River Basin from 2000 to 2040 and analyzed the characteristics of land use and habitat quality changes under scenarios of natural development (S1), ecological protection (S2), and urban expansion (S3). The results showed that in 2000, 2005, 2010, 2015, and 2020, the main land use types in the watershed were dryland and grassland, accounting for more than 72%. Paddy land, dryland, woodland, middle-coverage grassland, and unused land all showed decreasing trends, whereas all other land types showed increasing trends. Influenced by human activities and the environment, the watershed habitat quality was low, with 80% of the areas with middle to low grades, but the overall trend was rising. The spatial variability in habitat quality of the watershed was significant, with habitat quality improvements in the central and northern regions and continued deterioration around the cities in the southern and western parts. The spatial autocorrelation and aggregation of habitat quality in the watershed were strong, and future land use patterns in the study area had a significant relationship with human activities. Simulation of future scenarios revealed ecological conservation catalytic effects on habitat quality in the study area, whereas urban expansion deteriorated watershed habitat quality. This study could provide support for future ecological conservation decisions.

**Keywords:** logistic-CA-Markov model; InVEST model; land use; habitat quality; hotspot analysis

**Citation:** Fu, C.; Liu, Y.; Chen, Y.; Li, F.; Huang, J.; Huang, H. Simulation of Land Use Change and Habitat Quality in the Yellow River Basin under Multiple Scenarios. *Water* **2022**, *14*, 3767. <https://doi.org/10.3390/w14223767>

Academic Editor: Renato Morbidelli

Received: 17 October 2022

Accepted: 16 November 2022

Published: 19 November 2022

**Publisher's Note:** MDPI stays neutral with regard to jurisdictional claims in published maps and institutional affiliations.



**Copyright:** © 2022 by the authors. Licensee MDPI, Basel, Switzerland. This article is an open access article distributed under the terms and conditions of the Creative Commons Attribution (CC BY) license (<https://creativecommons.org/licenses/by/4.0/>).

## 1. Introduction

Habitat quality is the basis of ecosystem services, which refers to the ability of ecosystems to provide benefits to the survival, reproduction, and development for organisms. It can reflect, to a certain extent, the state of biodiversity in the region, which is the objective existence of essential properties in the ecological environment [1,2]. The habitat has social and ecological benefits for human and species survival [3]. However, with the development of the economy and societies, changes in land use mode, intensity, and patterns caused by large-scale human activities significantly impact the quality of biological habitats. These changes cause fragmentation, degradation, and even loss of local habitats, reducing habitat biodiversity and ecological service value, which will affect human well-being [4,5]. Therefore, exploring the relationship between land use and habitat quality, and simulating future changes in land use and habitat quality under different scenarios is significant for protecting regional biodiversity and sustainable land use.

Numerous studies have shown that habitat degradation due to land use change is a significant driver of biodiversity [6], and that land use change directly results from human-nature interactions [7]. In recent decades, land use change due to rapid global urbanization

has had profound impacts on habitat quality [8], as it affects the cycling processes of material and energy flows between habitat patches and alters the patterns and functions of regional habitat distribution [7]. The impact of land use on habitat quality will continue to deepen in the future due to increasing urbanization. Therefore, predicting the impact of land use change on habitat quality is an urgent task in coordinating sustainable land development and habitat conservation [8]. Nowadays, land use prediction models mainly include the FLUS model, CLUE-S model, CA-Markov model, and other models based on cellular automata. However, the FLUS model has difficulty reflecting the spatial differences in land use changes in different regions [9]. The CLUE-S model ignores the possibility of non-dominant land type transformations [10]. The CA-Markov model has had good results with predicting future land use. Abijith et al. [11] projected the land use of the Tamil Nadu for 2019–2030 to explore future urban growth scenarios under natural and anthropogenic pressures. Taking Beijing as an example, Yi et al. [12] predicted and optimized the land use changes in the study area in 2030, based on land adaptation evaluations to provide scientific references for land use planning. Wang et al. [13] simulated the LUCC of 29 towns in the Connecticut River Basin by OLR-CA-Markov (ordinary logistic regression-CA-Markov) and GWR-CA-Markov (geographically weighted regression-CA-Markov) methods to verify the advantages and disadvantages of the two methods.

Current research on habitat quality has focused on two aspects: habitat quality studies on species groups [14,15] and overall regional habitat quality studies [16,17]. During the study of individual species groups, the distribution data of species are mainly obtained through field monitoring, such as for giant pandas [18], tanager cranes [19], grassland Orthoptera communities [20], fish communities [21], and habitat quality studies on plant diversity [22], which is a difficult and expensive method of data collection and only suitable for small-scale regional studies. At the regional study scale level, the methods used mainly include nature reserves [23], urban scale [24], provincial scale [25], and watershed scale [26]. The methods studied mainly involve the InVEST model [27–29], MaxEnt model [19], FLUS model [30], and the combination of grid evaluation and landscape patterns [31]. The InVEST model applies to different regional scales, showing better ecological process integration and good spatial display effects [32], and its habitat quality module can quickly assess the impact of different threats and land use types on biodiversity [33]. Studies have shown that this model effectively assesses biodiversity and habitat quality [34–36].

The work mentioned above has promoted the study of regional habitat quality and provided a deeper understanding of the spatial and temporal variation of habitat quality, influencing factors, and conservation measures. However, there is still room for further research and deepening understanding. First, most of the studies on the Yellow River Basin have focused on some parts, such as its nature reserves, provinces, cities, or sub-basins, but there are still only a few studies that have examined the Yellow River Basin as a whole. Therefore, this study will examine the habitat quality of the Yellow River Basin, as a whole, to reveal the characteristics of land use and habitat quality changes in the entire basin. Second, under the circumstance that future land use is not easy to predict, especially on the time scale for studying environmental quality, researchers generally study habitat quality using the current land use pattern or changing trends in habitat quality from a historical perspective. There have been few studies on land use and habitat quality changes using different possible scenarios.

General Secretary Xi Jinping has repeatedly pointed out that the high-quality development of the Yellow River Basin “must adhere to the concept that lucid waters and lush mountains are invaluable assets, and adhere to ecological priority and green development” [37]. The Yellow River Basin is one of the regions with the most concentrated habitats in population, resources, and environment in China [38]; many animals and plants live and multiply here. However, its ecological environment is relatively fragile [39], facing ecosystem degradation, soil erosion, and various pollution problems. Environmental protection is the bottom line for the high-quality development of the Yellow River Basin, and an excellent ecological environment is the basis for the sustainable development of the

Yellow River Basin [40]. Therefore, research on the Yellow River Basin's habitat quality has become increasingly important. It is significant to study the impact of land use changes in this area on habitat quality. Based on previous research, this paper uses the improved Logistic-CA-Markov model to simulate future land use pattern of the Yellow River Basin under different scenarios. It selects the habitat quality module of the InVEST model to analyze the habitat quality of the Yellow River Basin from 2000 to 2040. Temporal and spatial evolution laws provide a scientific basis for protecting ecological diversity in the Yellow River Basin and the green development of regional ecology.

## 2. Materials and Methods

### 2.1. Study Site

The Yellow River is China's second largest river after the Yangtze River. It originated in the Tibetan Plateau Bayankara Mountain, and flows through 9 provinces, Qinghai, Sichuan, Gansu, Ningxia, Inner Mongolia, Shanxi, Shaanxi, Henan, and Shandong, and finally from Shandong into the Bohai Sea. It has a total length of 5464 km, and a basin area of 795,000 km<sup>2</sup>. The basin is extensive, and stretches across the Tibetan Plateau, Inner Mongolia Plateau, Loess Plateau, and Huang-Huai-Hai Plain from west to east [41]. The basin's annual average precipitation of 200~650 mm accounts for most of the basin, gradually increasing from northwest to southeast [42]. At the same time, the basin has low humidity and high evaporation, more hail, more sandstorms, and dust [43]. The basin's topography is complex and diverse, with the terrain being high in the west and low in the east, with a drop of 4480 m. There are many mountains in the west, with an average altitude of over 4000 m. The central area is relatively fragmented in geological structure and loose in soil texture. The eastern region mainly comprises the Yellow River alluvial plain, with a low average altitude, relatively complete urban construction, and a relatively developed economy (Figure 1).

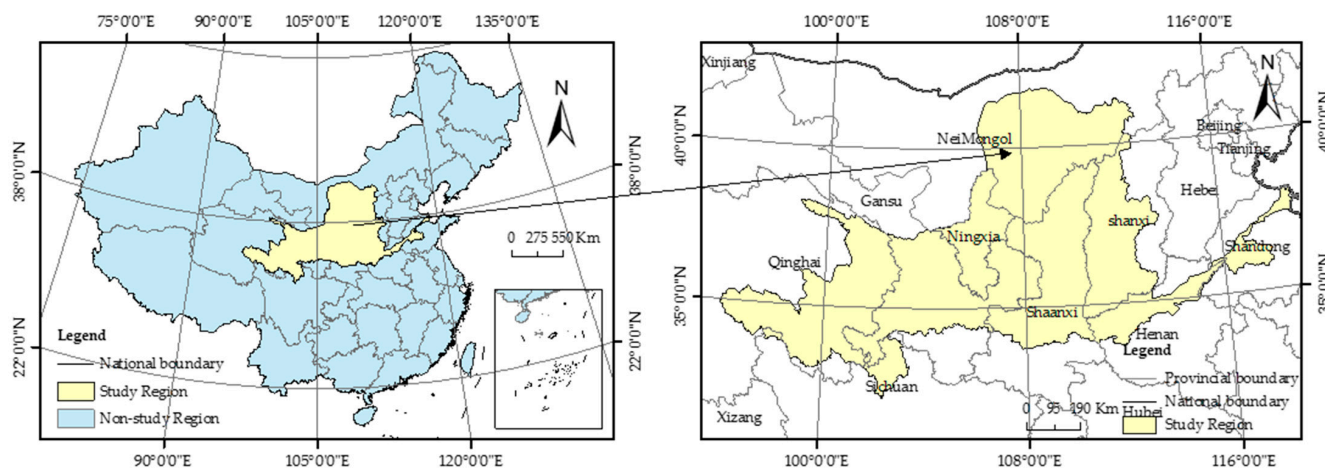


**Figure 1.** Location map of the Yellow River Basin.

### 2.2. Data Source and Processing

We used data from multiple sources (Table 1). The land use data from 2000 to 2020 comes from the Resource and Environmental Science Data Center of the Chinese Academy of Sciences. This product is based on the US Landsat series of remote sensing image data as the primary information source, which is obtained through manual visual interpretation, and is now widely used [44–46]. Considering the accuracy of the model and necessity of research, we reclassified the dataset using ArcGIS 10.2 (Environmental Systems Research Institute, Redlands, CA, USA) (Table 2).

**Table 1.** Input data for the improved Logistic-CA-Markov model and InVEST model.

Data	Data Source	Data Center URL
DEM data	National Cryosphere Desert Data Center	<a href="http://www.ncdc.ac.cn">http://www.ncdc.ac.cn</a> , accessed on 20 May 2022
Land use data (2000, 2005, 2010, 2015, and 2020), watershed boundaries, provincial and municipal boundaries, average annual precipitation, average annual temperature, soil sand content, population, and GDP	Resource and Environment Science and Data Center	<a href="https://www.resdc.cn/">https://www.resdc.cn/</a> , accessed on 22 May 2022
Water system, railroads, highways, national roads, and urban points	Geographical Information Monitoring Cloud Platform	<a href="http://www.dsac.cn/">http://www.dsac.cn/</a> , accessed on 25 May 2022

**Table 2.** Land use reclassification.

Reclassification	Original Land Types	Descriptions
Paddy field	Paddy field	Cultivated land with water source guarantee and irrigation facilities, which can be normally irrigated in ordinary years and used to grow rice, lotus root, and other aquatic crops, including the cultivated land with a rotation of rice and dry land crops.
Dry land	Dry land	Cultivated land without irrigation water source and facilities, relying on natural water to grow crops; cultivated land for dry crops with water source and irrigation facilities, which can be irrigated normally in ordinary years; cultivated land mainly for growing vegetables; leisure and rest areas for normal rotation.
Woodland	Woodland	Natural forests and artificial forests with canopy density higher than 30%, including timber forest, economic forest, shelter forest, and other woodland.
Shrub wood	Shrub wood	Low forest land and shrub land with a canopy density higher than 40% and height below 2 m.
Sparse wood	Sparse wood	The forest land with 10–30% canopy density.
Other woodland	Other woodland	Refers to the forest land, slash, nursery, and various gardens (orchard, mulberry garden, tea garden, hot planting forest garden, etc.).
High-coverage grassland	High-coverage grassland	Refers to the natural grassland, improved grassland, and mowed grassland covering more than 50%. This kind of grassland generally has good water conditions and dense grass coverage.
Middle-coverage grassland	Middle-coverage grassland	Natural grassland and improved grassland with 20–50% coverage. This type of grassland is generally lacking water and has sparse grass coverage.
Low-coverage grassland	Low-coverage grassland	Refers to natural grassland with 5–20% coverage. There is a shortage of grass moisture, grass is sparse, and the conditions for animal husbandry use are poor.
Water	Rivers and canals Lakes	Refers to natural or manually excavated rivers and land below the perennial water level of the trunk. The artificial channel includes the embankment.
	Reservoir ponds	Refers to the land below the perennial water level in the naturally formed ponding area.
	Reservoir pit	Refers to the land below the perennial water level in the artificially built water storage area.
	Permanent glacial snow	Land covered by glaciers and snow.

Table 2. Cont.

Reclassification	Original Land Types	Descriptions
Water	Mudflats	Refers to the tidal zone between the high tide and low tide levels of the coastal spring tide.
	Beach land	Refers to the land between the water level in the normal period and the water level in the flood period in the river and lake regions.
Urban land	Urban land	Refers to the construction areas of large cities, medium-sized cities, small cities, and counties and towns.
Rural settlements	Rural settlements	Refer to the rural residential areas independent of cities and towns.
Other construction land	Other construction land	Refers to the land used for factories and mines, large industrial zones, oil fields, salt farms, quarries, etc., as well as traffic roads, airports, and special land.
Unused land	Sandy	Refers to the land whose surface is covered with sand and vegetation coverage is below 5%, including desert, excluding desert in water system.
	Gobi	Refers to the land whose surface is mainly composed of crushed gravel and whose vegetation coverage is below 5%.
	Saline land	Refers to the land with saline alkali accumulation on the surface, few vegetation, and only strong saline alkali-resistant plants.
	Marshland	Refers to the land with flat and low-lying terrain, poor drainage, long-term humidity, seasonal or perennial water accumulation, and surface growth of hygrophytes.
	Bare land	Refers to the land with surface soil coverage and vegetation coverage below 5%.
	Bare rock texture	Refers to the land whose surface is rock or gravel and its coverage area is more than 5%.
	Other	Refers to other unused land, including alpine desert, tundra, etc.

In this paper, based on the actual habitat conditions and production and living conditions in the study area, we selected the DEM (Digital Elevation Model), slope, slope direction, GDP, population density, annual precipitation, average annual temperature, water system distance, road distance, urban distance, and soil sand content as the drivers of land use change. DEM data was provided by the National Cryosphere Desert Data Center. Slope and aspect were obtained based on DEM data using the Slope and Aspect functions of ArcGIS 10.2. GDP, population, soil sand content, average annual precipitation, and average annual temperature at a resolution of  $1 \times 1$  km were collected from the Resource and Environment Science and Data Center of the Chinese Academy of Sciences. The completed railways, highways, national roads, and river systems were obtained through the Geographic Information Monitoring Cloud Platform, and accessibility data was extracted through Euclidean distance. Then, we normalized all driving factors (Figure 2), which were used to participate in the production of the subsequent land use suitability atlas.

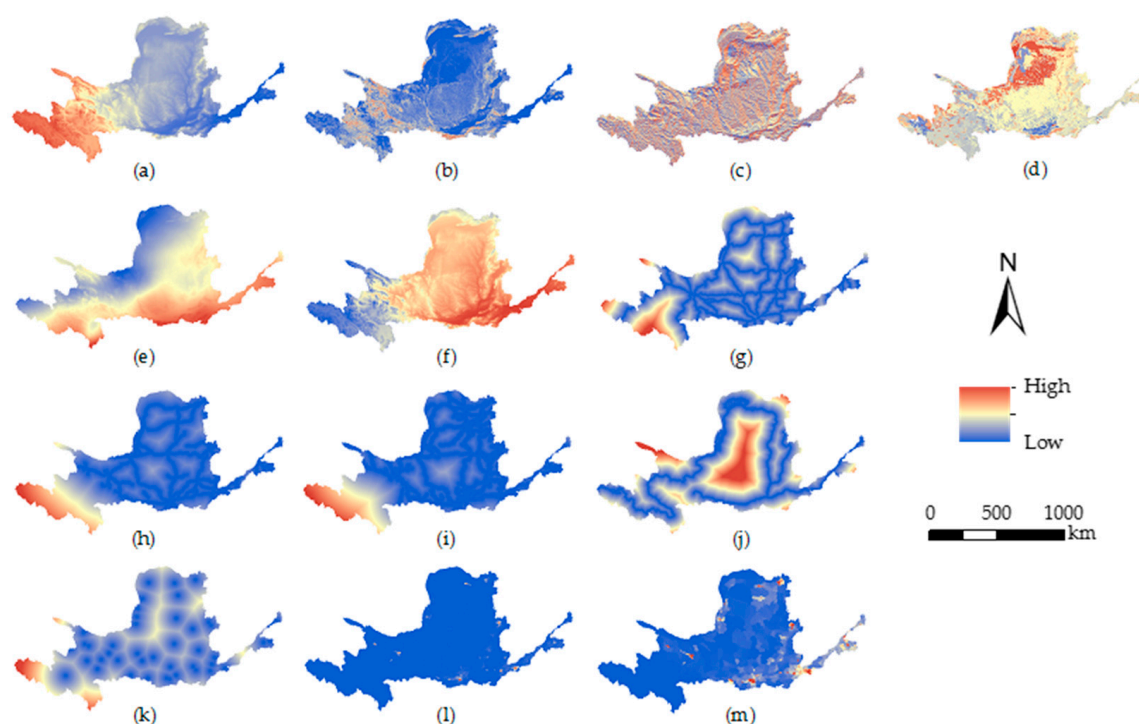


**Figure 2.** The main driving factors of land use change in Yellow River Basin: (a) elevation (m); (b) slope (degree); (c) aspect, in positive degrees from 0 to 359.9, measured clockwise from north; (d) soil sand content (%); (e) average annual precipitation (mm); (f) average annual temperature (°C); (g) distance to highway; (h) distance to motorway (m); (i) distance to railway (m); (j) distance to river (m); (k) distance to city (m); (l) population per km<sup>2</sup>; and (m) GDP per km<sup>2</sup>.

### 2.3. Methodology

#### 2.3.1. Logistic Regression Model

The logistic regression model is mainly used for binary or multi-category factor variable analysis, and is currently widely used in the study of driving forces of land use change [47]. The regression equation is as follows:

$$\log\left(\frac{P_i}{1 - P_i}\right) = \beta_0 + \beta_1 x_1 + \beta_2 x_2 + \dots + \beta_n x_n \quad (1)$$

In Equation (1),  $P_i$  is the probability of occurrence for land-use type  $i$  in each grid;  $x_1, x_2, x_3, \dots, x_n$  are driving factors that affect the land-use type transition;  $\beta_0$  is the intercept; and  $\beta_1, \beta_2, \beta_3, \dots, \beta_n$  are the regression coefficients. The relative operating characteristic (ROC) method proposed by Pontius [48] is usually used to verify the goodness of fit of the logistic regression model, and its value ranges from 0.5 to 1. The closer the value is to 1, the better the diagnostic effect is, and a value greater than 0.75 indicates that the accuracy of the regression fitting results is high and can meet the requirements. By examining the regression equations of each category and the driving factors (Table 3), we found that the ROC values were all greater than 0.8, indicating that the driving factors were reasonably selected in this paper.

**Table 3.** Logistic regression coefficients and ROC test results for each land use type in the Yellow River Basin.

Driving Factors	PF	DL	WL	SL	SW	OW	HCG	MCG	LCG	WA	UL	RS	OCL	UNL
DEM	0.0008	0.0005	−0.0001	0.0006	−0.0002	0.0007	0.0008	0.0003	0.0003	−0.0007	−0.0003	−0.0007	−0.0002	0.0003
Slope	−0.3463	−0.1123	0.2036	0.1086	0.0932	0.0096	0.0026	0.0321	−0.0043	−0.1257	−0.2606	−0.2319	−0.1181	−0.1162
Aspect	−0.0028	−0.0005	0.0005	0.0004	0.0006	0.0009	0.0007	−0.0001	0.0003	−0.0020	−0.0007	0.0002	−0.0007	0.0004
Soil sand content	0.0000	0.0001	0.0002	0.0005	0.0001	0.0038	0.0001	0.0002	0.0002	−0.0004	0.0001	0.0002	0.0001	0.0001
Precipitation	−0.0017	0.0001	0.0008	0.0004	0.0004	−0.0001	0.0003	−0.0002	−0.0005	−0.0002	−0.0002	0.0001	−0.0002	−0.0007
Temperature	0.1108	0.0265	−0.0091	−0.0010	−0.0140	0.0303	−0.0006	0.0029	0.0102	0.0023	0.0086	−0.0070	0.0029	0.0007
Distance to highway	0.0000	0.0000	0.0000	0.0000	0.0000	0.0000	0.0000	0.0000	0.0000	0.0000	0.0000	0.0000	0.0000	0.0000
Distance to motorway	0.0000	0.0000	0.0000	0.0000	0.0000	0.0000	0.0000	0.0000	0.0000	0.0000	0.0000	0.0000	0.0000	0.0000
Distance to railway	0.0000	0.0000	0.0000	0.0000	0.0000	0.0000	0.0000	0.0000	0.0000	0.0000	0.0000	0.0000	0.0000	0.0000
Distance to river	0.0000	0.0000	0.0000	0.0000	0.0000	0.0000	0.0000	0.0000	0.0000	0.0000	0.0000	0.0000	0.0000	0.0000
Distance to city	0.0000	0.0000	0.0000	0.0000	0.0000	0.0000	0.0000	0.0000	0.0000	0.0000	0.0000	0.0000	0.0000	0.0000
Population	0.0009	0.1846	−0.1955	−0.1925	−0.0793	−0.0984	−0.2785	−0.0343	−0.0048	0.0518	0.8679	0.3172	−0.6377	−0.2902
GDP	0.2388	0.0004	0.0004	0.0838	0.0003	0.0542	0.2754	0.0005	0.0003	0.0765	0.2534	0.0002	0.7553	0.4076
Intercept	−9.5158	−4.1372	−5.7165	−5.4361	−3.6803	−9.2983	−4.8519	−1.5534	−1.5715	−1.7194	−5.3449	−1.7856	−3.2506	−0.9849
ROC	0.9654	0.9319	0.9424	0.9196	0.9061	0.8950	0.8880	0.8905	0.8970	0.9257	0.9763	0.9350	0.9338	0.9311

Note: PF is paddy field; DL is dry land; WL is woodland; SL is shrub land; SW is sparse wood; OW is other woodland; HCG is high-coverage grassland; MCG is middle-coverage grassland; LCG is low-coverage grassland; WA is water; UL is urban land; RS is rural settlements; OCL is other construction land; and UNL is unused land.

### 2.3.2. Improved CA-Markov Model

The Markov model can predict the state of the event in the next period according to the state of the event in a certain period [49]. The key is to determine the probability of the event, which is a long-term prediction method [50]. The traditional Markov model in predicting future land use changes mainly depends on the transfer matrix of land use in two periods. The development of land use is also influenced by policies such as land use planning, which makes it difficult to simulate future land use, whereas the improved Markov model introduces the scenario weight matrix  $w_n$  based on the traditional model, and then the land use maps under different scenarios can be simulated by simply setting the appropriate scenario weight matrix. The improved Markov equation is as follows:

$$P_{(n)} = P_{(n-1)} \times P''_{ij} \quad (2)$$

$$P'_{ij} = P_{ij} \times w_n \quad (3)$$

$$P''_{ij} = \begin{bmatrix} \frac{1}{\sum_{n=1}^j P'_{1n}} & & \\ & \ddots & \\ & & \frac{1}{\sum_{n=1}^j P'_{in}} \end{bmatrix} P'_{ij} \quad (4)$$

In Equations (2)–(4),  $P_{ij} = \begin{bmatrix} P_{11} & \cdots & P_{1j} \\ \vdots & \ddots & \vdots \\ P_{i1} & \cdots & P_{ij} \end{bmatrix}$ ;  $w_n = \begin{bmatrix} w_1 & & \\ & \ddots & \\ & & w_n \end{bmatrix}$ ;  $n$  is the number of

land classes;  $P$  is the land-use transition probability matrix; its element  $P_{ij}$  is the transition probability of occurrence from type  $i$  to type  $j$ ; and  $0 \leq P_{ij} < 1$ ,  $\sum_{i=1}^n P_{ij} = 1$ ,  $P'_{ij}$  is the transfer matrix after changing the land class weights for  $P_{ij}$ . Using Equation (4), such that  $\sum_{i=1}^n P''_{ij} = 1$ ,  $P''_{ij}$  is obtained.

The cellular automata (CA) model is a discontinuous spatiotemporal dynamic simulation model with discrete time, space, and state, which can simulate complex events using relatively simple constraints [51]. The CA equation is as follows:

$$S_{(T)} = f[S_{(T-1)}, N] \quad (5)$$

In Equation (5),  $S$  is the set of finite and discrete cellular states,  $T$  and  $T - 1$  are adjacent to different moments,  $N$  is the cellular neighborhood range, and  $f$  is the state transition rule function of cellular interactions in the neighborhood range.

We used Kappa coefficients [52] to check the accuracy of the 2020 land use simulation results, and then projected future land use from 2025, 2030, 2035, and 2040 by equal interval projections [53].

### 2.3.3. Land Use Scenario Design

Scenario analysis aims to describe and analyze the various development possibilities and inform policy formulation by comparing the status of different development scenarios [54]. We summarize the policy orientation of national documents [55–58], and combined with existing studies, set three weighting values for different land use change scenarios (Table 4): (1) The natural development scenario (S1) is a continuation of the law of land use change from 2000 to 2020 and does not change the conversion rules in the land use category. (2) The ecological protection scenario (S2) is based on the ecological protection policy, which reduces the cultivated land area, increases the planting of forest land and grassland, and limits the speed of urban expansion. (3) The urban expansion scenario (S3) is simulated by increasing the growth rate of urban land and reducing the growth rate of ecological lands such as forests and grass.

**Table 4.** Scenario weighting matrix.

Scenario Type	Scenario Weight Matrix $w_n$ Value
S1	—
S2	Diag (0.95, 0.95, 1.2, 1.2, 1.2, 1.2, 1.2, 1.2, 1.1, 1, 0.85, 0.85, 0.85, 1)
S3	Diag (1, 1, 1, 0.9, 0.9, 0.9, 0.9, 0.9, 0.9, 1, 1.2, 1.2, 1, 1)

2.3.4. The InVEST Model

We used the Integrated Valuation of Environmental Services and Tradeoffs (InVEST) model to evaluate changes in habitat quality in the ecosystem. It can provide a scientific basis for decision-makers to weigh the benefits and impacts of human activities by simulating changes in the quantity and value of ecosystem services under different land cover scenarios [59]. The ‘‘Habitat Quality’’ module of the model calculates the spatial distribution of simulated habitat quality. The InVEST model equation is as follows [60]:

$$Q_{xy} = H_j \left[ 1 - \left( \frac{D_{ij}^z}{D_{xj}^z + kZ} \right) \right] \tag{6}$$

$$D_{xj} = \sum_{r=1}^R \sum_{y=1}^{Y_r} \left( \frac{\omega_r}{\sum_{r=1}^R \omega_r} \right) r_y i_{rxy} \beta_x S_{jr} \tag{7}$$

In Equations (6) and (7),  $Q_{xy}$  represents habitat quality;  $D_{xj}$  represents the degree of habitat degradation;  $H_j$  represents the habitat suitability of land use type  $j$ ;  $k$  is the half-saturation constant;  $Z$  is the normalized constant of the default parameters of the model;  $R$  represents the total threat sources and  $r$  represents one of the threat sources;  $Y_r$  refers to the sum of the grids on the  $r$  threat layer;  $\omega_r$  represents the weight of threat source  $r$ ;  $r_y$  is used to judge whether grid  $y$  is the source of threat source  $r$ ;  $i_{rxy}$  represents the distance impact function of threat source  $r$  in the habitat of grid  $x$  on grid  $y$ ; and  $\beta_x$  represents the protection of society, law, etc., which is not taken into consideration in this research.  $S_{jr}$  represents the sensitivity of habitat type  $j$  to threat source  $r$ , and the calculation is as follows [59]:

$$i_{rxy} = 1 - \frac{d_{xy}}{d_{rmax}} \tag{8}$$

$$i_{rxy} = \exp \left[ - \frac{2.99}{d_{rmax}} d_{xy} \right] \tag{9}$$

In Equations (8) and (9),  $d_{xy}$  represents the linear distance between grid  $x$  and  $y$ , and  $d_{rmax}$  represents the maximum impact distance of threat source  $r$ ; 1 indicates the ideal state.

Taking the actual situation in the study area into account, we selected five land types (paddy fields, drylands, urban land, rural settlements, and other construction land) as the definition of threat sources. We referred to the InVEST Model User’s Manual and combined the characteristics of the study area and relevant literature [61–64], assigning values to the sensitivity of each habitat to threat factors (Tables 5 and 6). We used the natural intermittent point grading method in ArcGIS 10.2 to grade habitat quality. This method classified habitat quality into five grades: lower (0~0.4), low (0.4~0.7), middle (0.7~0.8), high (0.8~0.95), and higher ( $\geq 0.95$ ).

**Table 5.** The maximum impact distance, weight, and attenuation type of threat sources.

Threat Source	Maximum Stress Distance (km)	Weight	Attenuation Type
Paddy field	6	0.5	Linear
Dry land	3	0.5	Linear
Urban land	10	1	Exponential
Rural settlements	5	0.6	Exponential
Other construction land	12	1	Exponential

**Table 6.** Habitat suitability and sensitivity to threats.

Type	Habitat Suitability	Sensitivity				
		Paddy Field	Dry Land	Urban Land	Rural Settlements	Other Construction Land
PF	0.4	0.3	1	0.5	0.7	0.1
DL	0.3	1	0.3	0.5	0.7	0.3
WL	1	0.7	0.8	1	0.85	0.6
SL	1	0.65	0.4	0.6	0.45	0.2
SW	1	0.6	0.85	1	0.9	0.65
OW	1	0.5	0.9	1	0.95	0.7
HCG	0.8	0.8	0.4	0.6	0.45	0.2
MCG	0.75	0.75	0.45	0.65	0.5	0.25
LCG	0.7	0.7	0.5	0.7	0.55	0.3
WA	0.9	0.6	0.2	0.9	0.75	0.7
UL	0	0	0	0	0	0
RS	0	0	0	0	0	0
OCL	0	0	0	0.7	0	0
UNL	0	0	0	0	0	0

Note: PF is paddy field; DL is dry land; WL is woodland; SL is shrub land; SW is sparse wood; OW is other woodland; HCG is high-coverage grassland; MCG is middle-coverage grassland; LCG is low-coverage grassland; WA is water; UL is urban land; RS is rural settlements; OCL is other construction land; and UNL is unused land.

### 2.3.5. Spatial Self-Correlation

To explore the spatially dependent associations of habitat quality within the Yellow River Basin, we conducted a spatial autocorrelation analysis of habitat quality in the basin. Moran’s I index revealed the global spatial autocorrelation characteristics of habitat quality in the study area, with a value range of [−1, 1]. The positive and negative magnitude of the value reflected its interconnected nature and significance. Z-values were used to test the significance of the Moran’s I index. When the Z-value is more significant than 2.58, it indicates a high degree of significance. The higher the Z-value, the greater the degree of agglomeration or dispersion. Local spatial autocorrelation reflected a certain attribute’s local spatial correlation characteristic. When the Moran’s  $I_i$  index value was greater than 0, it indicated high-high (H-H) or low-low agglomeration, whereas a value less than 0 indicated low-high (L-H) and high-low (H-L) agglomeration. The calculation process was completed in GeoDa 1.14 software. The calculation is as follows:

$$Moran's\ I = \frac{n \sum_{i=1}^n \sum_{j=1}^n w_{ij} (x_i - \bar{x})(x_j - \bar{x})}{(\sum_{i=1}^n \sum_{j=1}^n w_{ij}) \sum_{i=1}^n (x_i - \bar{x})^2} \tag{10}$$

$$Z_I = \frac{I - E[I]}{\sqrt{E[I^2] - E[I]^2}} \tag{11}$$

$$Moran's\ I_i = \frac{n(x_i - \bar{x}) \sum_{j=1}^n w_{ij}(x_j - \bar{x})}{\sum_{i=1}^n w_{ij}(x_j - \bar{x})^2} \tag{12}$$

In Equations (10)–(12),  $n$  is the number of spatial grids;  $x_i$  and  $x_j$  represent the observations on spatial grids  $i$  and  $j$ , respectively;  $\bar{x}$  is the average value; and  $w_{ij}$  is the spatial weight matrix.  $E[I] = -1/(n - 1)$ , representing the expectation index.

### 2.3.6. Cold-Spot and Hotspot Analysis

Cold- and hotspot analysis can be used to explore the non-random nature of element spatial distributions and detect hotspot areas where elements occur with high frequency.

Therefore, this method was used in this paper to analyze the study area’s cold- and hotspot areas of habitat quality. The formula is as follows [65]:

$$G_i = \frac{\sum_{j=1}^n w_{ij}x_j}{\sum_{j=1}^n x_j} \tag{13}$$

In Equation (13),  $G_i^*$  is the aggregation index of grid  $i$ ;  $w_{ij}$  is the transfer matrix between grid  $i$  and  $j$ ;  $x_i$  and  $x_j$  are the attribute values of the grid; and  $n$  is the total number of grids.

### 3. Results

#### 3.1. Land Use Change (2000–2020)

From 2000 to 2020, the main land use types in the study area were dryland and grassland (high-, middle-, and low-coverage grassland), accounting for more than 72%. The changes in different land use types were apparent (Figure 3), among which paddy fields, dryland, forested land, middle cover grassland, and unused land all showed decreasing trends. The net decrease in dryland was the largest (11,322 km<sup>2</sup>), with a net reduction of 5.35%, mainly due to the accelerated urbanization process and the policy of “returning farmland to grass and forest”. The net reduction rate of paddy fields was the largest, 16.71%, with an area of 1224 km<sup>2</sup>. Other lands showed increasing trends. Among them, the net growth area and net growth rate of other construction land were the highest, 5164 km<sup>2</sup> and 454.18%, respectively.

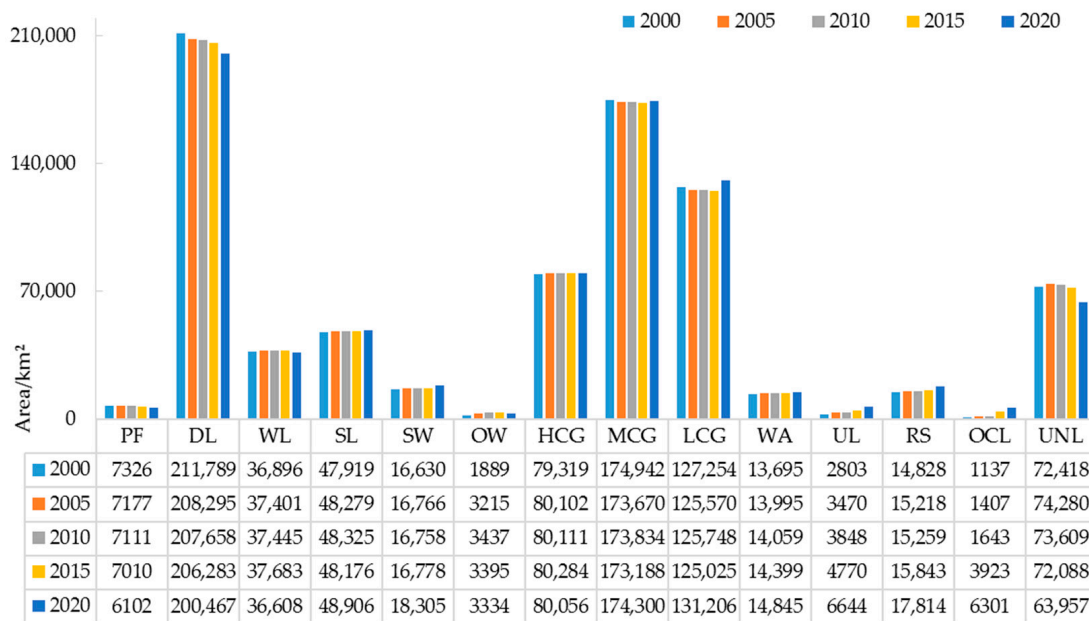


Figure 3. Land use change in the Yellow River Basin in 2000, 2005, 2010, 2015, and 2020.

From 2000 to 2020, the stable intensity of land types, in order from high to low, are urban land, rural settlements, woodland, dry land, paddy field, unused land, high-coverage grassland, middle-coverage grassland, low-coverage grassland, other construction land, shrub land, water, sparse woodland, and other woodland (Table 7). In 2020, 85.8% of urban land remained unchanged, and different land types were converted to urban land in different degrees, among which dryland had the largest inflow area of 2425 km<sup>2</sup>. Only 17.84% of other forest land remained unchanged, and the rest was converted to other land use types, with the most significant proportion converted to dryland at 35.31%.

**Table 7.** Land use transfer matrix of the Yellow River Basin between 2000 to 2020 (%).

		2020													
		PF	DL	WL	SL	SW	OW	HCG	MCG	LCG	WA	UL	RS	OCL	UNL
2000	PF	58.35	10.91	1.04	0.34	0.90	0.64	1.08	1.30	2.10	4.94	4.95	9.30	1.79	2.36
	DL	0.18	60.69	1.58	2.46	1.62	0.60	3.15	14.11	10.02	1.49	1.15	1.34	0.84	0.80
	WL	0.23	7.38	60.91	7.43	6.75	0.24	8.88	4.86	1.68	0.37	0.11	0.51	0.23	0.42
	SL	0.05	9.02	5.52	45.95	2.48	0.27	13.38	15.54	5.65	0.51	0.04	0.25	0.23	1.10
	SW	0.45	18.94	7.15	6.95	32.24	0.33	9.13	14.8	6.75	0.55	0.26	0.94	0.54	0.96
	OW	2.12	35.31	4.08	2.49	1.8	17.84	4.98	9.32	6.41	2.44	4.50	5.40	2.06	1.27
	HCG	0.06	7.69	4.08	8.08	2.07	0.16	54.46	11.12	5.85	0.88	0.11	0.60	0.37	4.48
	MCG	0.08	15.4	1.18	4.26	1.35	0.38	5.60	53.1	12.15	0.86	0.11	0.69	0.62	4.23
	LCG	0.15	16.85	0.6	2.26	0.98	0.3	3.56	15.18	51.45	0.96	0.16	0.77	0.81	5.96
	WA	2.12	19.50	1.22	1.47	0.80	0.37	3.86	8.93	8.84	42.49	1.09	2.33	1.23	5.76
	UL	0.32	2.89	0.86	0.21	1	0.29	0.50	1.32	0.93	1.71	85.8	2.82	1.32	0.04
	RS	2.47	3.81	0.94	0.71	0.73	0.63	2.2	6.49	4.43	2.08	3.03	69.76	1.55	1.17
	OCL	0.79	7.30	0.79	0.70	0.79	0.62	1.76	5.63	4.40	8.88	11.61	5.45	48.28	2.99
	UNL	0.25	3.29	0.54	0.92	0.33	0.11	4.97	12.62	16.5	1.55	0.07	0.37	0.92	57.57

Note: PF is paddy field; DL is dry land; WL is woodland; SL is shrub land; SW is sparse wood; OW is other woodland; HCG is high-coverage grassland; MCG is middle-coverage grassland; LCG is low-coverage grassland; WA is water; UL is urban land; RS is rural settlements; OCL is other construction land; and UNL is unused land.

Construction land (urban land, rural settlements, and other construction land) in the eastern region of the study area continues to expand, mainly in the form of large areas of paddy fields, drylands, and middle- and low-coverage grasslands converted to construction land. Among them, 1175 and 15,542 km<sup>2</sup> of paddy fields and drylands were converted into construction land, mainly in central cities and surrounding towns, represented by the conversion of paddy fields into drylands and urban land around Luoyang City and Zhengzhou City (Figure 4). The conversion of middle- and low-coverage grassland into construction land were 2494 and 2209 km<sup>2</sup>, respectively. The conversion of dryland and grassland (high-, middle-, and low-coverage grassland) was frequent. The transformation process was mainly scattered in the plains of the basin, where 57,762 km<sup>2</sup> of arable land was converted to grassland, but 54,489 km<sup>2</sup> of arable land was also converted to dryland, resulting in little overall change in the arable land area, which would decline by a total of 5.73% (12,546 km<sup>2</sup>) by 2020. The area of water has been expanding and expanded by 8.40% (1150 km<sup>2</sup>) in 20 years. The largest converted area was from dry land to water, reaching 3151 km<sup>2</sup>, followed by middle-coverage grassland and low-coverage grassland, 1499 and 1221 km<sup>2</sup>, respectively. The conversion process mainly occurred around the water system in the study area, with the most conversion at the mouth of the Yellow River. The forest land changed less, and woodland areas only increased by 3819 km<sup>2</sup> in 20 years; however, there was a large area of grassland conversion to woodland, with 6070, 16,732, 5244, and 1178 km<sup>2</sup> of grassland transformed into woodland, shrub land, sparse wood, and other woodland, respectively.

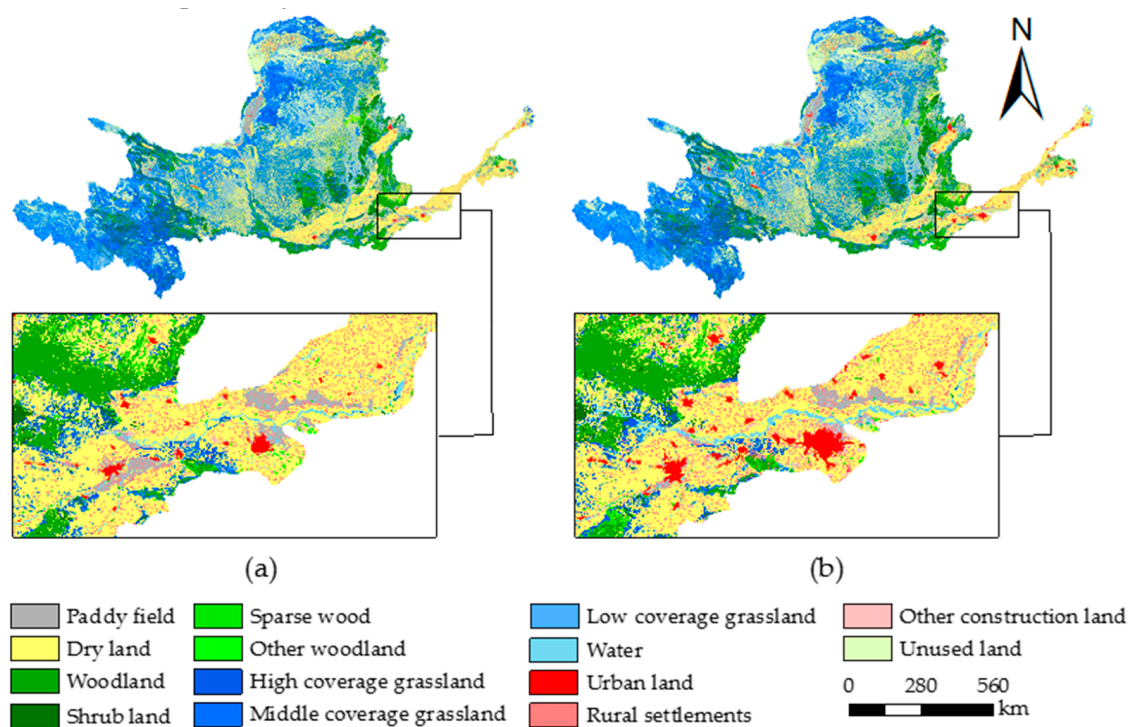


**Figure 4.** Spatial distribution of land use type in Yellow River Basin: (a) 2000 and (b) 2020.

### 3.2. Prediction of Land Use Change (2025–2040)

#### 3.2.1. Accuracy Assessment

The verification results showed that the Kappa coefficient of simulation results and actual land use in 2020 was 0.8336. By comparing land use types (Table 8), we could see that the differences between the 2020 simulation map and the actual status quo map in 2020 were relatively small for each land use type, with 11 land use types having an error of less than 5%. The errors of other woodland, urban land, and other construction land areas were relatively more significant. However, they also met the simulation requirements because the areas were small and the locations on the map were the same (Figure 5).

**Table 8.** Accuracy test of land use simulation in 2020.

Type	Actual Area (km <sup>2</sup> )	Simulated Area (km <sup>2</sup> )	Error (%)	Type	Actual Area (km <sup>2</sup> )	Simulated Area (km <sup>2</sup> )	Error (%)
PF	6102	6254	2.49	MCG	174,300	173,724	−0.33
DL	200,467	201,414	0.47	LCG	131,206	128,388	−2.15
WL	36,608	36,048	−1.53	WA	14,845	15,153	2.07
SL	48,906	50,039	2.32	UL	6644	6031	−9.23
SW	18,305	18,739	2.37	RS	17,814	18,547	4.11
OW	3334	3758	12.72	OCL	6301	5744	−8.84
HCG	80,056	79,649	−0.51	UNL	63,957	65,772	2.84

Note: PF is paddy field; DL is dry land; WL is woodland; SL is shrub land; SW is sparse wood; OW is other woodland; HCG is high-coverage grassland; MCG is middle-coverage grassland; LCG is low-coverage grassland; WA is water; UL is urban land; RS is rural settlements; OCL is other construction land; and UNL is unused land.

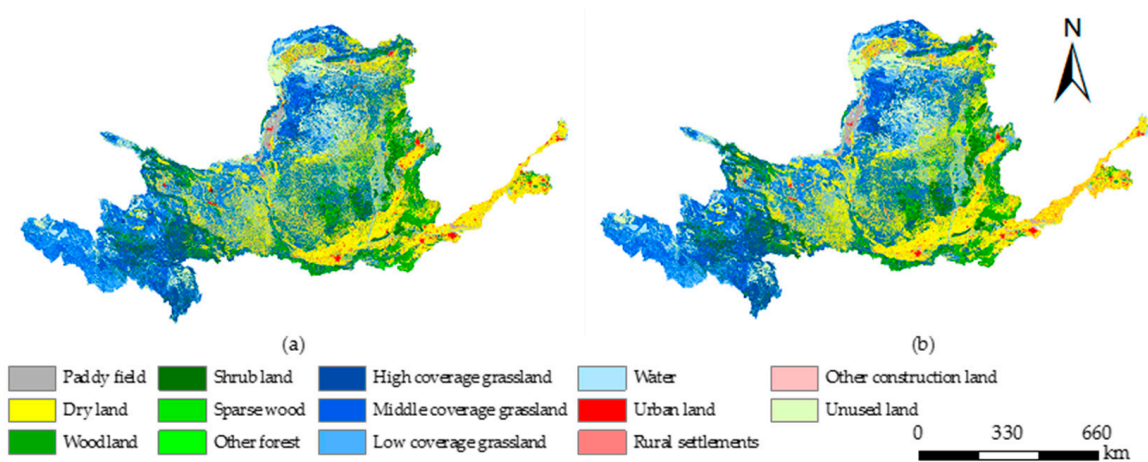


**Figure 5.** Current situation and simulation map of land use and cover in the Yellow River Basin in 2020: (a) land use map in 2020 and (b) simulated land use map in 2020.

### 3.2.2. Multi-Scenario Simulation

The multi-scenario land use simulation projections (Figure 6) showed that overall land use pattern is relatively consistent from 2025 to 2040, but local differences are more pronounced.

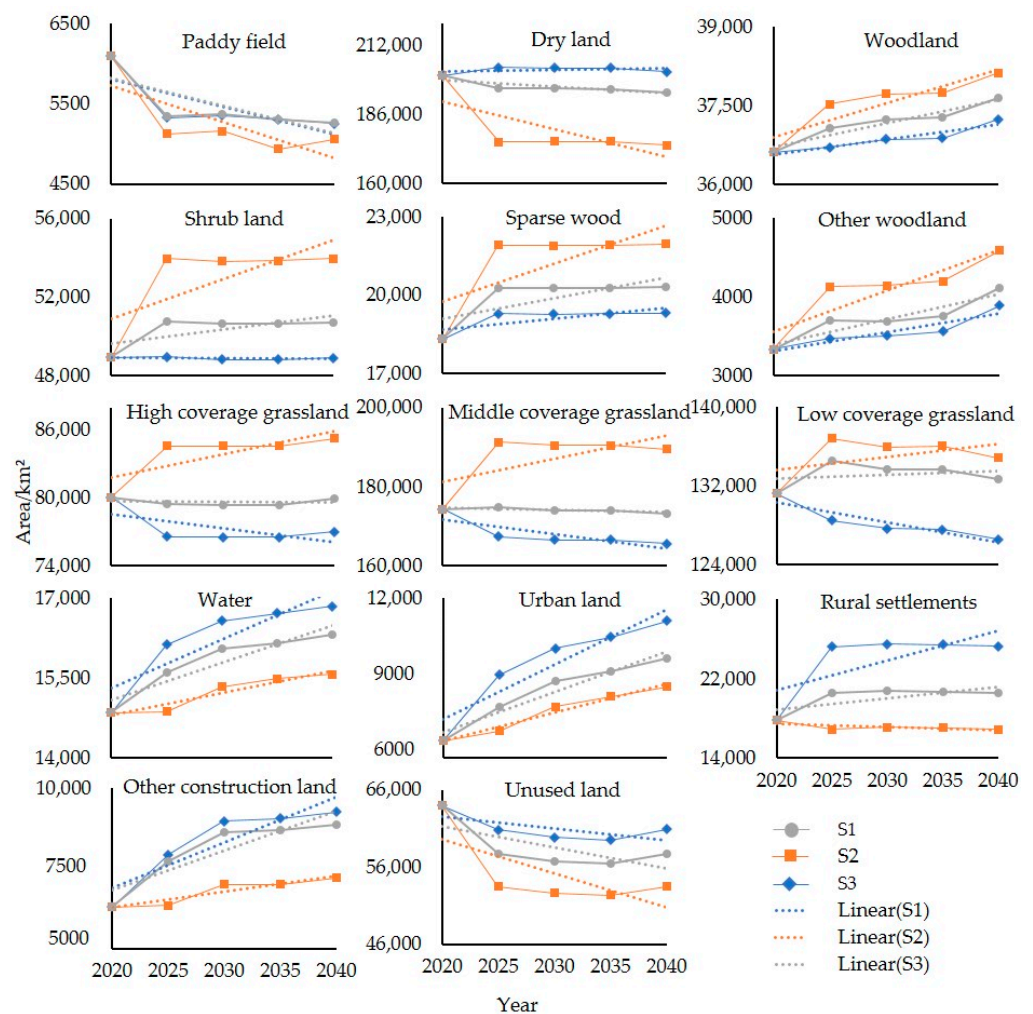


**Figure 6.** Prediction map of land use in different scenarios in 2025, 2030, 2035, and 2040.

Paddy fields and dryland are mainly distributed in the southern plains of the basin and around the river valleys; under S2, they decline significantly ( $52.1 \text{ km}^2/\text{a}$ ,  $1299.5 \text{ km}^2/\text{a}$ ). Woodland generally shows an increasing trend, pronounced in S2 ( $280.28 \text{ km}^2/\text{a}$ ). The grassland area varies significantly in different contexts. Under S2, grasslands (high-, middle-, and low-coverage grasslands) show an increasing trend. However, under S1 and S3, grasslands show a decreasing trend, with the most significant decrease in S3, with high-, middle-, and low-coverage grasslands decreasing by 0.19, 0.25, and 0.18% per year on average. The water area shows a slow increase, with the most significant increase in S3 ( $99.70 \text{ km}^2/\text{a}$ ). Urban land is concentrated in urban clusters in the southern and eastern parts of the study area. Under S3, the area of urban land, rural residential land, and other construction land will continue to grow. However, the growth rate of urban land is significantly higher than that of rural residential land, with urban land, rural residential land, and other construction land increasing by 67.47, 41.69, and 46.90%, respectively. Under S2, the expansion of urban land in the south and east of the study area is remarkably restrained; in 2040, urban land expands by only 30%.

### 3.3. Habitat Quality (2000–2020)

#### 3.3.1. Spatial and Temporal Variation of Habitat Quality

The habitat quality index is between 0 and 1, and the larger the value, the better the habitat quality. The study area's habitat quality table (Table 9) from 2000 to 2020 was obtained. The habitat quality of the study area rose first and then declined. Specifically, it increased by 0.02, 0.08, and 0.94% from 2000 to 2005, 2005 to 2010, and 2015 to 2020, respectively; in the period 2010–2015, habitat quality decreased by 0.20%, but the overall habitat quality in the study area showed an increasing trend, and the standard deviation increased period by period, indicating that the difference in habitat quality between raster cells was spatially expanding.

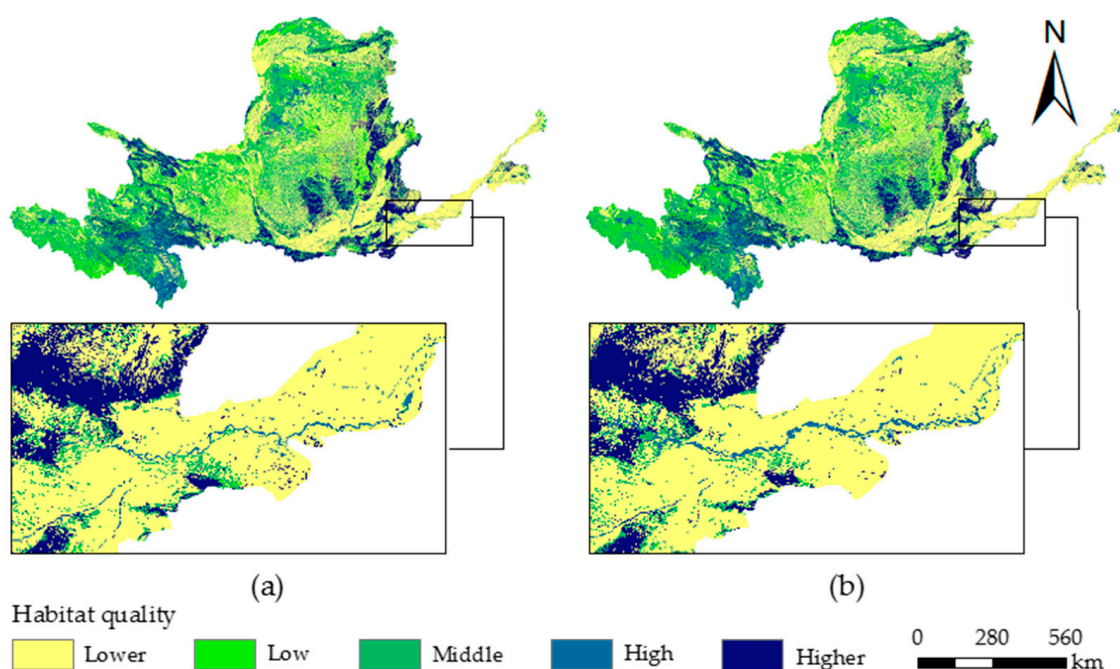
**Table 9.** Habitat quality of the Yellow River Basin in 2000, 2005, 2010, 2015, and 2020.

Year	Habitat Quality	Standard Deviation
2000	0.57405	0.30899
2005	0.57416	0.31137
2010	0.57465	0.31138
2015	0.57347	0.31266
2020	0.57887	0.31285

Through statistics and reclassification of habitat quality, we obtained changes in habitat quality classes in the Yellow River Basin (Table 10, Figure 7). From 2000 to 2020, the areas with low habitat quality and below accounted for more than 53.47% of the study area. The areas with middle habitat quality and below was more than 80% of the total area of the study area, indicating that the overall level of habitat quality in the study area was low. The spatial distribution of habitat quality was similar to land use distribution. The areas with high habitat quality were mainly distributed in forest land (woodland, shrub land, sparse wood, and other woodland) and high-coverage grassland areas. Furthermore, the areas with low habitat quality were mainly distributed in construction land, dry land, and unused land areas. Those with low habitat quality and below decreased from 54.09 to 53.47%; those with high habitat quality and above decreased from 19.97 to 19.75%, indicating the polarization of habitat quality in the study area had eased.

**Table 10.** Changes in habitat quality grades in the Yellow River Basin in 2000, 2005, 2010, 2015, and 2020.

Habitat Quality Grade	Index Range	Area Share (%)				
		2000	2005	2010	2015	2020
Lower	0~0.4	38.36	38.31	38.22	38.32	37.25
Low	0.4~0.7	15.73	15.52	15.55	15.46	16.22
Middle	0.7~0.8	25.94	25.96	26.01	26.23	26.78
High	0.8~0.95	7.19	7.14	7.13	6.88	6.50
Higher	0.95~1	12.78	13.06	13.10	13.11	13.25

**Figure 7.** Habitat quality in the Yellow River Basin: (a) 2000 and (b) 2020.

The areas with lower habitat quality were mainly located in the Hetao Plain, Ningxia Plain, Weihe Plain, and the downstream area of the basin, areas with intense human activity, mainly construction and arable land. The overall decrease in this area was 0.14% (450.8 km<sup>2</sup>/a) per year, indicating that the poor-quality areas in the study area were gradually restored. The areas with low habitat quality were mainly located in the western plateau of the study area and the Ordos Plateau and Maowusu Sandy area in the north-central part of the study area, which is mainly low-coverage grasslands. The habitat quality was low mainly because the habitat suitability of grassland was higher than that of cropland, construction land, and unused land, but lower than that of water and forest land. This led to a low classification of habitat quality, and the average annual growth of this area was 0.17% (197.6 km<sup>2</sup>/a) over 20 years. The areas with middle habitat quality showed an increasing trend from period to period, mainly in the western and north-central areas of the Basin, where the ecological environment was more complex, made up of primarily high- and middle-coverage grassland areas, with an annual increase of 0.16%, on average (340.25 km<sup>2</sup>/a). The areas with high habitat quality were in southern Qinghai, northern Sichuan, and southern Inner Mongolia, mainly high-coverage grassland and water areas, which showed a decreasing trend year by year, with an average annual decrease of 0.48% (278 km<sup>2</sup>/a). The suitability of all woodlands was 1, which made the areas with higher habitat quality mainly concentrated in woodlands, watersheds, and the junction, and the area increased period by period, with an average annual increase of 0.18% (190.95 km<sup>2</sup>/a), indicating that the afforestation in China was effective.

In general, the habitat quality of the study area improved significantly over the past 20 years. The habitat quality in the central and northern parts of the Basin has improved to varying degrees. However, with the development of the social economy and acceleration of urbanization, the habitat quality of various urban sites in the study area has continued to deteriorate. The patches of low value habitat quality areas tend to spread, especially in the middle and lower reaches of the Basin, and provincial capital cities such as Xi'an and Zhengzhou are severe. Meanwhile, due to the construction of road traffic and other facilities, cities in the eastern part of the Basin tend to form urban clusters, which makes the inter-urban habitats continuously divided and habitat quality fragmented to different degrees. The expansion of cities and towns brought about by human activities remains the most prominent factor causing ecological damage.

### 3.3.2. Spatial Transfer Analysis of Habitat Quality Grades

The statistical transfer matrix of habitat quality classes was obtained by superimposing the distribution maps of 2000 and 2020 (Table 11, Figure 8). In 2020, 66.03% of the areas with lower habitat quality remained lower quality, 10.97% had changed to low grade, and 15.55% converted to middle grade, with a conversion area of 44,288 km<sup>2</sup> and the conversion process occurring mainly in eastern Gansu Province and the eastern and western regions of Shaanxi Province. In addition, 2.49% converted to high grade, and 4.95% to higher grade, and the relatively small area converted was mainly because the conditions in areas with lower habitat quality were deplorable and could only be improved with human intervention. Of the areas with low habitat quality, 24.70% were converted to lower grade, mainly distributed in central Gansu Province, southern Ningxia, and northern and eastern Shaanxi Province. 51.45% were not converted, 16.94% were converted to the middle grade, mainly in the western plateau areas of the study area, and 2.76 and 4.14% were converted to high and higher grade, respectively. Of the areas with middle habitat quality, 21.11 and 10.99% were converted to lower and low grades, respectively, with the conversion occurring mainly in the eastern region of Gansu Province, 55.40% were not transformed, and 8.94% were transformed to the higher grade, which was mainly distributed in the eastern region of Qinghai, the western region of Gansu Province, and the central region of Shaanxi Province. Of the areas with high habitat quality, 49.68% of the areas were not converted, 13.11 and 6.97% were converted to lower and low grades, respectively, 18.10% was converted to middle grade, and 9.83% was converted to higher grade. The areas that were converted to higher grade were mainly concentrated in the eastern part of Qinghai, the western part of Gansu, and the northern part of Sichuan Province. Of the areas with higher habitat quality, 18.10, 4.42, and 12.62% of the higher habitat quality areas changed to the middle, low, and lower grades, respectively, whereas 60.03% did not change and remained at higher grades. The areas that changed from higher to lower were mainly located around cities, indicating that urban expansion posed a serious threat to their surrounding ecological environment.

**Table 11.** Habitat quality grade transfer matrix between 2000 to 2020 (%).

		2020				
		Lower	Low	Middle	High	Higher
2000	Lower	66.03 *	10.97	15.55	2.49	4.95
	Low	24.70	51.45 *	16.94	2.76	4.14
	Middle	21.11	10.99	55.40 *	3.56	8.94
	High	13.11	6.97	20.41	49.68 *	9.83
	Higher	12.62	4.42	18.10	4.83	60.03 *

Note: \* denotes unconverted parts; other data denote converted parts.

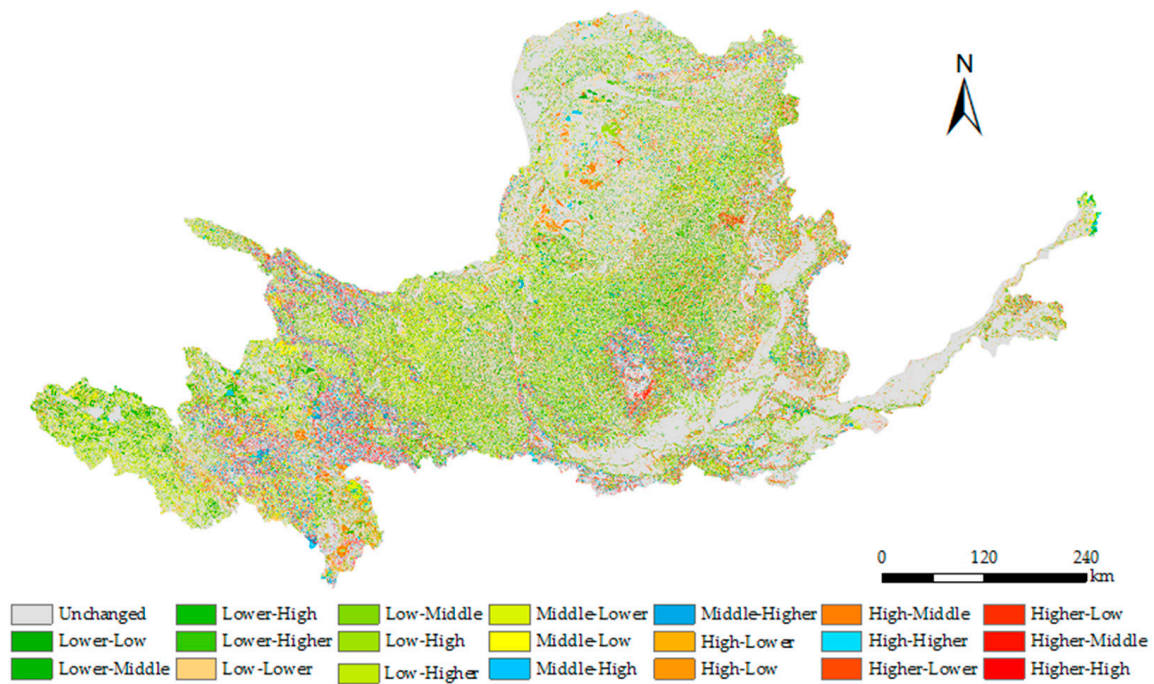


**Figure 8.** Spatial distribution of changes in habitat quality grade in the Yellow River Basin between 2000 to 2020.

### 3.3.3. Autocorrelation Analysis of Habitat Quality

By using three spatial weights (Queen, Rook, and k), we found that the Moran’s I index of habitat quality in 2020 was 0.742, 0.778, and 0.771, respectively (Figure 9), indicating that the habitat quality in the Yellow River Basin presented a strong autocorrelation in space.

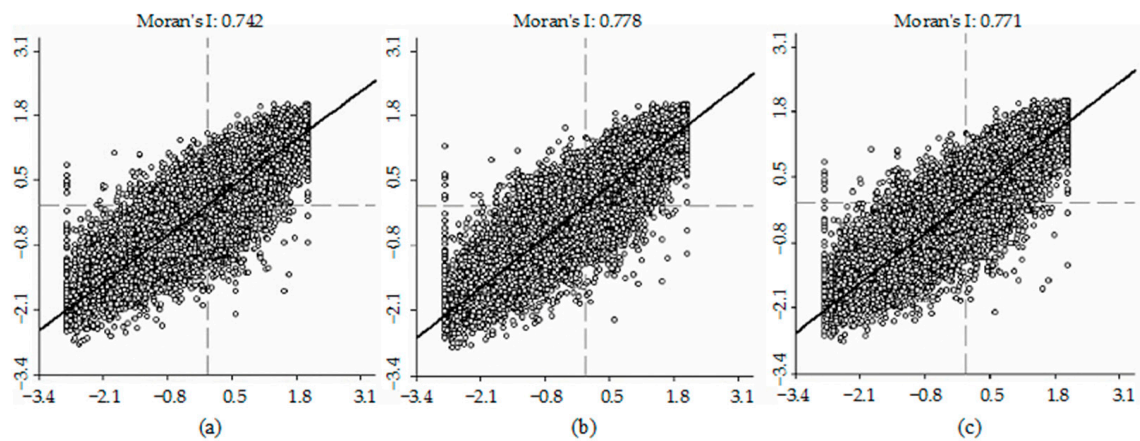


**Figure 9.** Scatterplot of Moran’s I index of habitat quality in 2020: (a) Queen-nearest neighbor; (b) Rook-nearest neighbor; and (c) K-nearest neighbor.

In using Rook-NN spatial weights, when the *p*-value is 0.001, the *z*-values are much bigger than 2.58, indicating that a solid spatial aggregation occurs in the Yellow River Basin. However, the global Moran’s I index of habitat quality in the Yellow River from 2000 to 2020 did not change much (Table 12), with differences between 0.771 and 0.778. The degree of aggregation showed a fluctuating trend, increasing, then decreasing, then increasing again, with the highest degree of spatial aggregation in 2020.

**Table 12.** Moran’s I index of habitat quality in the Yellow River Basin in 2000, 2005, 2010, 2015, and 2020.

Year	Moran’s I	p-Value	Z-Value
2000	0.771	0.001	199.5075
2005	0.775	0.001	197.1992
2010	0.774	0.001	196.3750
2015	0.773	0.001	196.3672
2020	0.778	0.001	195.2524

In the LISA (Local Indicators of Spatial Association) clustering map (Figure 10), the distribution of aggregates was relatively similar but varied locally. As shown in Table 13, the Not Significant area decreased from 63.77% in 2000 to 63.31% in 2020, and the Not Significant area in the west gradually changed to the “H-H” type. The main reason was that a large amount of unused land in this area was converted into grassland, promoting the flow of energy and material in the ecosystem. The “H-H” type aggregation area was mainly concentrated in the western and central parts of the watershed and around the “L-L” type in the east, which showed slight fluctuations and small overall change. The “L-L” type was mainly concentrated in the northern and southeastern regions of the Basin. The proportion of this region increased from 17.36% in 2000 to 17.89% in 2020, mainly dry land, unused land, and construction land (urban land, rural settlements, and other construction land), with a poorer ecological environment and more challenging to change. The proportion of “L-H” and “H-L” gathering areas was deficient, accounting for less than 0.5%, scattered in various parts of the Basin.

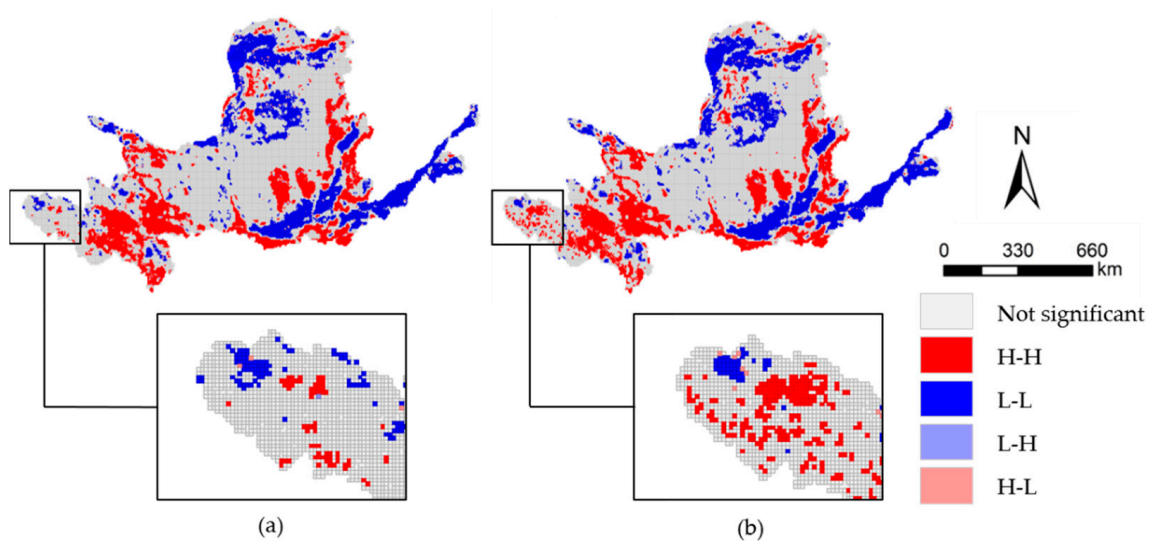


**Figure 10.** Local spatial autocorrelation clustering of habitat quality in the Yellow River Basin: (a) 2000 and (b) 2020.

**Table 13.** Clustering statistic of the local Moran’s I<sub>i</sub> for habitat quality (%).

Year	2000	2005	2010	2015	2020
Not Significant	63.77	63.76	63.67	63.65	63.31
H-H	18.33	18.22	18.25	18.27	18.30
L-L	17.36	17.50	17.55	17.53	17.89
L-H	0.23	0.23	0.22	0.24	0.15
H-L	0.31	0.29	0.31	0.31	0.35

### 3.3.4. Cold-Spot and Hotspot Analysis of Habitat Quality

We used 2020 as an example to reflect the spatial clustering of habitat quality in the study area (Figure 11). According to results of the cold-spot and hotspot analysis, there were apparent cold-spots and hotspots in the habitat quality of the Yellow River Basin. The distribution characteristics were “hot in the upper reaches, crossed by hot and cold in the middle, and cold in the lower reaches”. The distribution of cold-spots and hotspots was closely related to land use. The cold-spots were mainly distributed in the study area’s northern, central, and southern regions, mainly comprised of dry land, unused land, and construction land. In contrast, the hotspots were concentrated in the study area’s western plateau and eastern grassland and forest land areas.

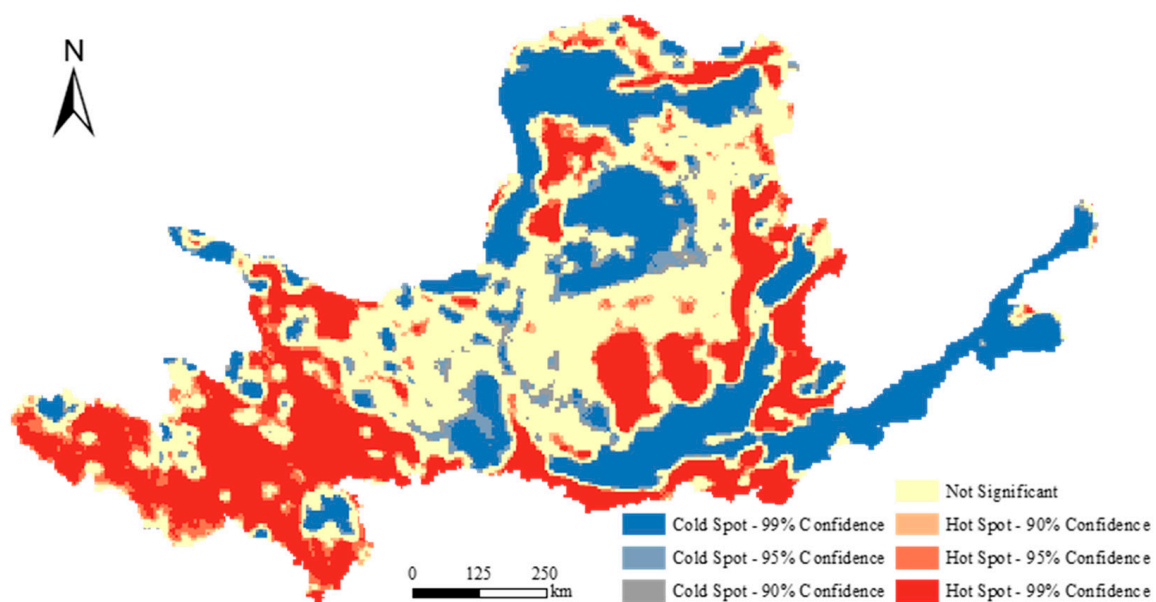


**Figure 11.** Habitat quality “Cold and hot spot” analysis in the Yellow River Basin in 2020.

### 3.4. Habitat Quality in Multiple Scenarios (2025–2040)

The habitat quality of the basin is closely related to its land use. Based on the projected land use, we simulated the spatial and temporal changes in habitat quality in the Yellow River Basin for 2025, 2030, 2035, and 2040 under different scenarios (Table 14). From the time scale, the habitat quality in the study area showed an increasing trend under the natural development and ecological protection scenarios, with an increase of 0.04 and 0.18%/a, respectively, which is the same as the overall change trend from 2000 to 2020. Under S2, the trend of increasing habitat quality was 2.69% higher than that of S1, which effectively improved the habitat quality of the study area. However, under S3, the habitat quality of the study area would continue to deteriorate, and the habitat quality index decreased by 0.09%/a, which was 2.55% lower than S1 and 5.20% lower than that of S2. From the spatial scale, the spatial distribution characteristics of habitat quality in the study area were consistent among the three scenarios. However, the distribution was closely related to land use. The eastern and southern urban construction sites and central low-coverage grassland areas in the study area were mainly of lower and low habitat quality. In contrast, the high and higher habitat quality was mainly distributed in the western hills and central woodland areas.

**Table 14.** Habitat quality of the Yellow River Basin under different scenarios in 2025, 2030, 2035, and 2040.

Year	Habitat Quality		
	S1	S2	S3
2025	0.58208	0.59430	0.57044
2030	0.58256	0.59954	0.56938
2035	0.58264	0.59970	0.56941
2040	0.58360	0.59990	0.56872

To further understand the habitat quality of the study area under different scenarios, we counted the percentage of habitat quality grades under different future scenarios (Figure 12). Under S1, the area with lower habitat quality will slowly increase in the next 20 years, rising from 36.44 to 36.64% of watershed area; areas with low and middle grades will gradually decrease, accounting for 16.40 and 24.33% of the entire watershed, respectively. At the same time, areas with high and higher habitat quality will slightly increase in the next 20 years, and areas with high and higher habitat quality will account for 22.64% of the whole study area in 2040. Under S2, the area with lower habitat quality will show some fluctuation, but the overall trend is decreasing, and will account for 32.86% of the overall area in 2040. The area with low and middle grades show a decreasing trend, accounting for 43.17% of the study area in 2040; the areas with high and higher grades show an increasing trend period by period, accounting for 23.96% of the overall study area in 2040. Under S3, the areas with lower grades increase period by period and account for 38.78% of the entire study area in 2040; the areas with low and middle grades decrease period by period and account for 38.93% of the study area in 2040. The areas with high and higher grades increase period by period and account for 22.3% of the study area in 2040.

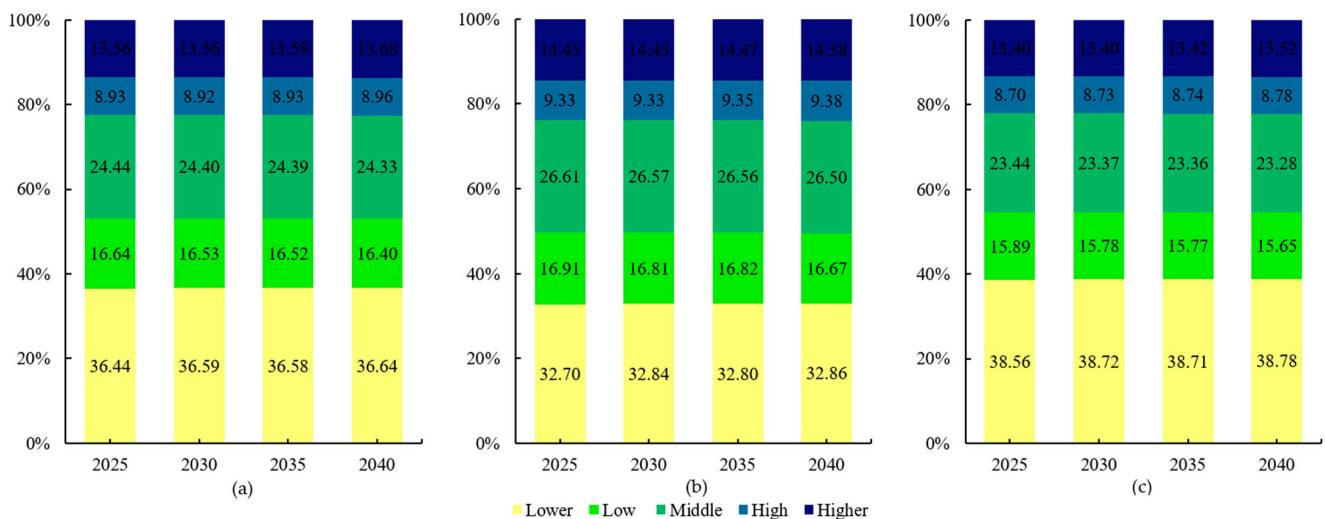


**Figure 12.** Proportion of habitat quality grades under different scenarios in 2025, 2030, 2035, and 2040: (a) natural development scenario; (b) ecological protection scenario; and (c) urban expansion scenario.

Ecological conservation positively contributes to habitat quality in the study area, whereas urban expansion reduces regional habitat quality. In 2040, S2 reduces the area of low and lower grades by 3.78% and improves the area of high and higher grades by 1.32% compared with S1, whereas in the S3, the area of lower habitat quality expands by 2.14%, and areas of high and higher grades decreased by 0.34%. Ecological conservation remains the critical way to improve regional habitat quality, whereas expanding built-up land is a significant factor in the deterioration of habitat quality.

## 4. Discussion

### 4.1. Interpretation of Land Use Change

According to the study results, the land use pattern in the study area has changed significantly in the past 20 years, with dryland and grassland being the primary land use types in this area. The conversion of dryland to grassland and forestland is significant, mainly due to the policies of “returning farmland to grassland” and “returning farmland to the forest” in the Loess Plateau. Implementing these policies has dramatically increased the area of grassland and forest land by replanting cultivated land formed by reclaiming mountains and forests into grassland [39]. However, scholars have different opinions on the main driving factors of the grassland area in the study area. Guo [66] believes that human activities are the main factor causing this area’s change in vegetation coverage. Mao [67] believes that the main factors in this area are social factors, and that the implementation of national policies played a significant role in driving and facilitating the process; in contrast, he claims that the impact of human activities is relatively small. However, Shahid Naeem [68] claims that precipitation contributed the most to the restoration of vegetation cover in the region. In the future, this question deserves more in-depth research.

In the three scenarios, the spatial distribution of land use in the future study area was the same, but in some areas, the land use type changed significantly. Under S1, the changes in various land use categories were relatively stable, and the development situation was the same as in 2000, 2005, 2010, 2015, and 2020. Under S2, grassland and forest land rose faster, whereas urban land, rural settlements, and other construction land expanded significantly slower. Under S3, the expansion rate of construction land in various cities accelerated significantly, and the area of rural settlements and other construction land also increased substantially, especially in eastern cities and rural areas. The main reason is that, with the development of the economy and society, people’s demand for land is increasing, which occupies a large amount of cultivated land around towns and rural areas, and the eastern plain will inevitably be affected as a cultivated land area. Ecological protection can effectively curb the problem of encroaching on cultivated land, and can also improve the coverage of regional vegetation. However, implementing environmental conservation measures while improving the regional ecological environment may impact the economical production of the study area. At the same time, expanding towns and cities may negatively impact the local ecological environment. Therefore, S1 and S2 had some contradictions in some areas. In the future, weighing up the relationship between economic development and ecological protection will be an important research direction.

### 4.2. Response of Habitat Quality to Land Use Change

From 2000 to 2020, the overall habitat quality in the study area showed a fluctuating trend of rising first, then falling, and then rising again; spatially, it showed the distribution characteristics of “high in the west and low in the east”, which is consistent with Yang [69], Song [70], and Liu et al. [71]’s research results. Local land use change mainly depends on implementing environmental protection policies and town expansion. Frequent human activities can change the regional land use pattern and thus affect the regional habitat quality. The distribution of habitat quality in the study area showed strong topographic distribution characteristics, and areas with better habitat quality were mainly concentrated in mountainous woodlands. The areas with average habitat quality were mainly concentrated in the highland grassland areas, which were more restricted for socio-economic development and had lower intensity of human activities, making their habitat quality more stable. The areas with low and lower habitat quality were mainly concentrated around the plains and waters with an excellent topographic environment because the natural conditions in the area were suitable for growing food crops and human life. This made a large amount of arable land, and construction land expansion led to a generally low level of habitat quality in the region and frequent transitions in habitat quality classes.

According to the predictions of the three future scenarios, it was found that under the ecological conservation scenario, the increase in the area of grassland and woodland and

decrease in the growth rate of urban construction land would lead to an increase in the regional habitat quality. In contrast, under S3, the growth rate of grassland and woodland decreases, and construction land area expands rapidly, leading to a decrease in the overall growth rate of habitat quality and even a decrease in habitat quality. These results are consistent with the findings of Ding et al. [8].

The study found that most of the decline in biodiversity and habitat quality was associated with urban expansion [8]. In contrast, most local increases in habitat quality depended on implementing environmental protection policies. During 2000–2020, habitat quality continued to improve in the western and northern regions of the basin, whereas the southeastern region showed a deterioration. This was mainly due to the establishment of the Sanjiangyuan Nature Reserve at the source of the Yellow River and the implementation of the “grazing and grass restoration project”, which has significantly increased the growth rate and area of vegetation in the region [72,73]. This has improved the regional habitat quality, and is consistent with the results of Yang [74]. Similarly, in the Maowusu sandy area in the north-central part of the Basin, implementing environmental protection policies, such as afforestation, has led to a yearly increase in greenery and improvements in habitat quality in the region. However, in the southeastern plain area, from 2000 to 2020, with the socioeconomic development, the study area had experienced an accelerated urbanization rate. Urban land has expanded by 137.0%, and construction land has expanded by 454.2% in 20 years, and the construction of various transportation facilities has continuously eroded the ecological environment, making the habitat in the area fragmented. There has been more degradation of the habitat around the city. The area of low-grade habitat quality in urban built-up areas is expanding. This increase in areas of urban land and rural settlements remains the main reason for the deterioration of local habitat quality.

#### *4.3. The Merits and Limitations of This Study*

In this study, the adaptation factors selected using the Logistic regression analysis model improved the objectivity of land use prediction. The improvement in the CA-Markov model makes it easier to set future scenarios, and the simulated land use was tested for accuracy with a kappa coefficient of 0.8336, which indicated high accuracy, suggesting that this model has strong applicability in the Yellow River Basin. The improved Logistic-CA-Markov and InVEST models were integrated to analyze the Yellow River Basin’s land use pattern and habitat quality for a long time series from 2000 to 2020. The study showed the importance of ecological conservation. The spatial and temporal changes in land use and habitat quality under the three scenarios of natural development, ecological conservation, and urban expansion from 2025 to 2040 were also simulated, which is essential for ecological conservation policies and urban planning studies in the study area. However, for future scenario setting, better policy quantification is needed as it can make the scenario matrix setting less objective; improving this process will lead to a more objective scenario weight matrix and improve the simulation effect. In addition, although our research results have specific reference value, the habitat quality in the study area was influenced by human and natural factors. The InVEST model has certain limitations, as it only considers the influence of nature and lacks consideration of human factors. Finally, in this study, the grid used was  $1 \times 1$  km. Considering the availability of data and the large size of the study area, the choice of scale could be explored in more depth.

#### *4.4. Policy Recommendations*

The Yellow River Basin is not only an important ecological barrier in the north of China, but also a traditional agricultural area in China, with a massive plantation and agricultural livestock industry at this stage, and the scale of commercial agricultural production is daily expanding [75]. The Yellow River Basin has effectively managed desert and sand in recent years, but the arable land area has significantly declined. In the future, it will be necessary to continuously optimize agricultural production methods and improve agricultural production efficiency based on maintaining the red line of arable

land. For urban areas in the watershed, caution should be taken against unreasonable urban sprawl and prevent the destruction of the environment in exchange for the economy, leading to continued deterioration in habitat quality. At the same time, urban planning and transportation planning in the eastern part of the study area should be developed in conjunction with ecological protection to reduce the risk of regional habitat fragmentation due to the emergence of urban agglomerations.

## 5. Conclusions

Based on the land use data from 2000 to 2020, this study analyzed the Yellow River Basin's land use and habitat quality using the improved Logistics-CA-Markov and InVEST models and predicted the Basin's land use and habitat quality from 2025 to 2040 under multiple scenarios. The conclusions are as follows:

(1) From 2000 to 2020, dryland and grassland were the primary land use types in the study area, accounting for more than 72%. Paddy land, dryland, forested land, middle-coverage grassland, and unused land all showed decreasing trends, whereas the other land categories show increasing trends. The overall pattern of land-use projections under the different scenarios was relatively consistent, but local differences were more pronounced. The ecological protection scenario substantially inhibited the expansion of urban land in the south and east of the Basin. In contrast, the urban expansion scenario accelerated land expansion for construction;

(2) From 2000 to 2020, habitat quality in the basin showed an upward trend, but at a low level, with areas with average or below grades making up 80% of the total area. There were differences in the spatial distribution of habitat quality, with the northern and central regions of the Basin showing varying degrees of improvement in habitat quality. In contrast, the southern and western cities of the Basin showed continuous deterioration. With the construction of transport facilities, there was a tendency for urban agglomerations to form in the eastern part of the Basin, which has led to constant fragmentation of the ecological environment between cities and varying degrees of habitat quality, with urban expansion brought about by human activity remaining the biggest factor affecting habitat quality;

(3) Habitat quality in the study area had strong spatial autocorrelation and aggregation. Cold-spots of habitat quality were mainly in the northern and southern parts of the watershed, concentrated in drylands, unused land, and built-up land; hotspots were mainly in the western plateau and the eastern grassland and woodland areas of the watershed;

(4) Ecological conservation had a significant positive effect on the habitat quality of the watershed, whereas urban expansion reduced the habitat quality of the watershed. According to our prediction, in 2040, S2 would reduce the area of poor and poor habitat quality by 3.78% compared with S1. Under S2, the area of lower habitat quality was 2.14% more than in S1, and the high and higher-grade area was 0.34% less.

**Author Contributions:** Conceptualization, C.F. and Y.L.; methodology, Y.L.; software, Y.L.; validation, Y.L., Y.C. and F.L.; formal analysis, C.F.; investigation, J.H. and H.H.; resources, C.F.; data curation, Y.L.; writing—original draft preparation, Y.L.; writing—review and editing, C.F.; visualization, Y.C.; supervision, C.F.; project administration, J.H.; funding acquisition, C.F. All authors have read and agreed to the published version of the manuscript.

**Funding:** This research was supported by the National Social Science Foundation of China, and the fund approval number is 18BGL187.

**Data Availability Statement:** The data used in this study are available upon request from the corresponding author.

**Conflicts of Interest:** The authors declare no conflict of interest.

## References

- Zhu, S.; Li, L.; Xing, L.; Wu, G.; Guo, H.; Wang, X.; Bao, G. Impact of the villages on habitat quality of Yunnan snub-nosed monkey in northwest Yunnan. *Acta Ecol. Sin.* **2022**, *42*, 1213–1223.
- Chu, L.; Zhang, X.-R.; Wang, T.-W.; Li, Z.-X.; Cai, C.-F. Spatial-temporal evolution and prediction of urban landscape pattern and habitat quality based on CA-Markov and InVEST model. *Yingyong Shengtai Xuebao* **2018**, *29*, 4106–4118. [[CrossRef](#)] [[PubMed](#)]
- Mengist, W.; Soromessa, T.; Feyisa, G.L. Landscape change effects on habitat quality in a forest biosphere reserve: Implications for the conservation of native habitats. *J. Clean. Prod.* **2021**, *329*, 129778. [[CrossRef](#)]
- Wang, C.; Chang, Y.; Hou, X.; Liu, Y. Temporal and Spatial Evolution Characteristics of Habitat Quality in Jiaodong Peninsula based on Changes of Land Use Pattern. *J. Geo-Inf. Sci.* **2021**, *23*, 1809–1822.
- Zhong, L.; Wang, J. Evaluation on effect of land consolidation on habitat quality based on InVEST model. *Trans. Chin. Soc. Agric. Eng.* **2017**, *33*, 250–255.
- Otto, C.R.; Roth, C.L.; Carlson, B.L.; Smart, M.D. Land-use change reduces habitat suitability for supporting managed honey bee colonies in the Northern Great Plains. *Proc. Natl. Acad. Sci. USA* **2016**, *113*, 10430–10435. [[CrossRef](#)]
- Dai, L.; Li, S.; Lewis, B.J.; Wu, J.; Yu, D.; Zhou, W.; Zhou, L.; Wu, S. The influence of land use change on the spatial-temporal variability of habitat quality between 1990 and 2010 in Northeast China. *J. For. Res.* **2018**, *30*, 2227–2236. [[CrossRef](#)]
- Ding, Q.; Chen, Y.; Bu, L.; Ye, Y. Multi-Scenario Analysis of Habitat Quality in the Yellow River Delta by Coupling FLUS with InVEST Model. *Int. J. Environ. Res. Public Health* **2021**, *18*, 2389. [[CrossRef](#)]
- Ji, Y.; Jia, L.; Yang, L.; Li, Y.; Dong, Q. Spatio-temporal Evolution and Prediction Analysis of Habitat Quality in Yulin City Coupled with InVEST-PLUS Model. *J. Soil Water Conserv.* **2022**, *37*, 1–10.
- Qiao, Z.; Jiang, Y.Y.; He, T.; Lu, Y.S.; Xu, X.L.; Yang, J. Land use change simulation: Progress, challenges, and prospects. *Acta Ecol. Sin.* **2022**, *42*, 5165–5176.
- Abijith, D.; Saravanan, S. Assessment of land use and land cover change detection and prediction using remote sensing and CA Markov in the northern coastal districts of Tamil Nadu, India. *Environ. Sci. Pollut. Res.* **2021**, 1–13. [[CrossRef](#)] [[PubMed](#)]
- Yi, Y.; Zhang, C.; Zhu, J.; Zhang, Y.; Sun, H.; Kang, H. Spatio-Temporal Evolution, Prediction and Optimization of LUCC Based on CA-Markov and InVEST Models: A Case Study of Mentougou District, Beijing. *Int. J. Environ. Res. Public Health* **2022**, *19*, 2432. [[CrossRef](#)] [[PubMed](#)]
- Wang, H.; Stephenson, S.R.; Qu, S. Modeling spatially non-stationary land use/cover change in the lower Connecticut River Basin by combining geographically weighted logistic regression and the CA-Markov model. *Int. J. Geogr. Inf. Sci.* **2019**, *33*, 1313–1334. [[CrossRef](#)]
- Green, D.B.; Bestley, S.; Corney, S.P.; Trebilco, R.; Lehodey, P.; Hindell, M.A. Modeling Antarctic Krill Circumpolar Spawning Habitat Quality to Identify Regions With Potential to Support High Larval Production. *Geophys. Res. Lett.* **2021**, *48*, e2020GL091206. [[CrossRef](#)]
- Pugesek, G.; Crone, E.E. Contrasting effects of land cover on nesting habitat use and reproductive output for bumble bees. *Ecosphere* **2021**, *12*, e03642. [[CrossRef](#)]
- Jia, Y.; Yu, D.; Wang, M.; Liu, B.; Ma, L. Spatio-Temporal Evolution and Correlation Analysis of Landscape Pattern and Habitat Quality in Tai'an City. *J. Northwest For. Univ.* **2022**, *37*, 229–237.
- Yang, G.; Zhang, H.; Li, J.; Guo, D.; Zhang, X. Spatial-temporal evolution and its influencing factors of habitat quality in Pingshuo mining area based on RFFLUS-InVEST-Geodetector coupling model. *J. Shaanxi Norm. Univ. Nat. Sci. Ed.* **2021**, *49*, 106–115.
- Wang, Y.; Lan, T.; Deng, S.; Zang, Z.; Zhao, Z.; Xie, Z.; Xu, W.; Shen, G. Forest-cover change rather than climate change determined giant panda's population persistence. *Biol. Conserv.* **2022**, *265*, 109436. [[CrossRef](#)]
- Wu, Q.; Wang, L.; Zhu, R.; Yang, Y.; Jin, H. Nesting habitat suitability analysis of red-crowned crane in Zhalong Nature Reserve based on MAXENT modeling. *Acta Ecol. Sin.* **2016**, *36*, 3758–3764.
- Fumy, F.; Kämpfer, S.; Fartmann, T. Land-use intensity determines grassland Orthoptera assemblage composition across a moisture gradient. *Agric. Ecosyst. Environ.* **2021**, *315*, 107424. [[CrossRef](#)]
- Cote, D.; Gregory, R.S.; Morris, C.J.; Newton, B.H.; Schneider, D.C. Elevated habitat quality reduces variance in fish community composition. *J. Exp. Mar. Biol. Ecol.* **2013**, *440*, 22–28. [[CrossRef](#)]
- Triantafyllidis, V.; Zotos, A.; Kosma, C.; Kokkotos, E. Effect of land-use types on edaphic properties and plant species diversity in Mediterranean agroecosystem. *Saudi J. Biol. Sci.* **2020**, *27*, 3676–3690. [[CrossRef](#)] [[PubMed](#)]
- Cao, M.; Cai, Y.; Zhang, L.; Xu, J. Temporal and spatial variation of typical ecosystem services in Wolong Nature Reserve. *Acta Ecol. Sin.* **2021**, *41*, 9341–9353.
- Han, Y.; Zhang, Q.; Zhang, S.; Yin, L. Optimizing the Habitat Quality of the East Lake Scenic Area in Wuhan. *Chin. Landsc. Archit.* **2021**, *37*, 95–100.
- Liang, X.; Yuan, L.; Ning, L.; Song, C.; Cheng, C.; Wang, X. Spatial pattern of habitat quality and driving factors in Heilongjiang Province. *J. Beijing Norm. Univ. Nat. Sci.* **2020**, *56*, 864–872.
- Li, Z.; Zhang, Y. Spatiotemporal Evolution of Ecosystem Services in the Main and Tributaries of Weihe River Basin Based on InVEST Model. *J. Soil Water Conserv.* **2021**, *35*, 178–185.
- Wang, H.; Tang, L.; Qiu, Q.; Chen, H. Assessing the Impacts of Urban Expansion on Habitat Quality by Combining the Concepts of Land Use, Landscape, and Habitat in Two Urban Agglomerations in China. *Sustainability* **2020**, *12*, 4346. [[CrossRef](#)]

28. Zhang, H.; Li, S.; Liu, Y.; Xu, M. Assessment of the Habitat Quality of Offshore Area in Tongzhou Bay, China: Using Benthic Habitat Suitability and the InVEST Model. *Water* **2022**, *14*, 1574. [[CrossRef](#)]
29. Berta Aneseyee, A.; Noszczyk, T.; Soromessa, T.; Elias, E. The InVEST Habitat Quality Model Associated with Land Use/Cover Changes: A Qualitative Case Study of the Winike Watershed in the Omo-Gibe Basin, Southwest Ethiopia. *Remote Sens.* **2020**, *12*, 1103. [[CrossRef](#)]
30. Li, Y.; Duo, L.; Zhang, M.; Wu, Z.; Guan, Y. Assessment and Estimation of the Spatial and Temporal Evolution of Landscape Patterns and Their Impact on Habitat Quality in Nanchang, China. *Land* **2021**, *10*, 1073. [[CrossRef](#)]
31. Ao, Y.; Jiang, L.; Bai, Z.; Yang, X.; Zhang, L. Comprehensive evaluation of land ecological quality in the Yellow River Basin based on Grid-GIS. *Arid Land Geogr.* **2022**, *45*, 164–175.
32. Li, M.; Zhou, Y.; Xiao, P.; Tian, Y.; Huang, H.; Xiao, L. Evolution of Habitat Quality and Its Topographic Gradient Effect in Northwest Hubei Province from 2000 to 2020 Based on the InVEST Model. *Land* **2021**, *10*, 857. [[CrossRef](#)]
33. Xu, L.; Chen, S.S.; Xu, Y.; Li, G.; Su, W. Impacts of Land-Use Change on Habitat Quality during 1985–2015 in the Taihu Lake Basin. *Sustainability* **2019**, *11*, 3513. [[CrossRef](#)]
34. Hack, J.; Molewijk, D.; Beißler, M.R. A Conceptual Approach to Modeling the Geospatial Impact of Typical Urban Threats on the Habitat Quality of River Corridors. *Remote Sens.* **2020**, *12*, 1345. [[CrossRef](#)]
35. Wang, B.; Cheng, W. Effects of Land Use/Cover on Regional Habitat Quality under Different Geomorphic Types Based on InVEST Model. *Remote Sens.* **2022**, *14*, 1279. [[CrossRef](#)]
36. Lee, D.-j.; Jeon, S.W. Estimating Changes in Habitat Quality through Land-Use Predictions: Case Study of Roe Deer (*Capreolus pygargus tianschanicus*) in Jeju Island. *Sustainability* **2020**, *12*, 10123. [[CrossRef](#)]
37. Xi, J.P. Speech at the Symposium on Ecological Protection and High-quality Development in the Yellow River Basin. *Qiushi J.* **2019**, *20*, 1–3.
38. Deng, X.; Yang, K.; Shan, J.; Dong, S.; Zhang, W.; Guo, R.; Tan, M.; Zhao, P.; Li, Y.; Miao, C.; et al. Urban agglomeration and industrial transformation and development in the Yellow River Basin. *J. Nat. Resour.* **2021**, *36*, 273–289. [[CrossRef](#)]
39. Yin, D.; Li, X.; Li, G.; Zhang, J.; Yu, H. Spatio-Temporal Evolution of Land Use Transition and Its Eco-Environmental Effects: A Case Study of the Yellow River Basin, China. *Land* **2020**, *9*, 514. [[CrossRef](#)]
40. Renquan, H. The Spatiotemporal Changes and Grey Relational Analysis of High-quality Development Level in the Yellow River Basin: An Empirical Research Based on the Data from 2000–2018. *Ecol. Econ.* **2022**, *38*, 62–70.
41. Yang, J.; Xie, B.; Zhang, D.; Chen, J. Soil erosion and its temporal-spatial variation in the Yellow River Basin based on the InVEST model. *J. Lanzhou Univ. Nat. Sci.* **2021**, *57*, 650–658.
42. Zhang, R.; Wang, Y.; Chang, J.; Li, Y. Response of land use change to human activities in the Yellow River Basin based on water resources division. *J. Nat. Resour.* **2019**, *34*, 274–287. [[CrossRef](#)]
43. Yang, J.; Xie, B.-P.; Zhang, D.-G. Spatio-temporal variation of water yield and its response to precipitation and land use change in the Yellow River Basin based on InVEST model. *Yingyong Shengtai Xuebao* **2020**, *31*, 2731–2739. [[CrossRef](#)] [[PubMed](#)]
44. Li, Y.; Liu, C.; Liu, X.; Liang, K.; Bai, P.; Feng, Y. Impact of the Grain for Green Project on the Land Use/Cover Change in the Middle Yellow River. *J. Nat. Resour.* **2016**, *31*, 2005–2020.
45. Wang, Z.; Wang, Z.; Zhang, B.; Lu, C.; Ren, C. Impact of land use/land cover changes on ecosystem services in the Nenjiang River Basin, Northeast China. *Ecol. Process.* **2015**, *4*, 11. [[CrossRef](#)]
46. Pan, Y.; Chen, Y.; Zhang, X.; Cao, F.; Sun, Z.; Du, X.; Zhao, X. Spatiotemporal changes analysis of land desertification sensitivity in Ningxia, China. *J. Beijing Norm. Univ. Nat. Sci.* **2020**, *56*, 582–590.
47. Rong, Y.; Zhang, H.; Wang, Y. Assessment on Land Use and Biodiversity in Nanjing City Based on Logistic-CA-Markov and InVEST Model. *Res. Soil Water Conserv.* **2016**, *23*, 82–89.
48. Pontius, R.G.; Schneider, L.C. Land-cover change model validation by an ROC method for the Ipswich watershed, Massachusetts, USA. *Agric. Ecosyst. Environ.* **2001**, *85*, 239–248. [[CrossRef](#)]
49. Zhang, X.; Zhou, J.; Li, M. Analysis on spatial and temporal changes of regional habitat quality based on the spatial pattern reconstruction of land use. *Acta Geogr. Sin.* **2020**, *75*, 160–178.
50. Mumtaz, F.; Tao, Y.; de Leeuw, G.; Zhao, L.; Fan, C.; Elnashar, A.; Bashir, B.; Wang, G.; Li, L.; Naeem, S.; et al. Modeling Spatio-Temporal Land Transformation and Its Associated Impacts on land Surface Temperature (LST). *Remote Sens.* **2020**, *12*, 2987. [[CrossRef](#)]
51. Chang, H.; He, G.; Wang, Q.; Li, H.; Zhai, J.; Dong, Y.; Zhao, Y.; Zhao, J. Use of sustainability index and cellular automata-Markov model to determine and predict long-term spatio-temporal variation of drought in China. *J. Hydrol.* **2021**, *598*, 126248. [[CrossRef](#)]
52. Abbas, Z.; Jaber, H.S. Accuracy assessment of supervised classification methods for extraction land use maps using remote sensing and GIS techniques. In *Materials Science and Engineering Conference Series*; Iop Publishing: Bristol, UK, 2020; Volume 745, p. 012166.
53. Li, Y.; Chang, J.; Wang, Y.; Liu, Q.; Fan, J.; Ye, D. Land use simulation and prediction in the Yellow River Basin based on CA-Markov model. *J. Northwest A&F Univ. Nat. Sci. Ed.* **2020**, *48*, 107–116.
54. Gao, X.; Yang, L.; Li, C.; Song, Z.; Wang, J. Land use change and ecosystem service value measurement in Baiyangdian Basin under the simulated multiple scenarios. *Acta Ecol. Sin.* **2021**, *41*, 7974–7988.
55. The Communist Party of China Central Committee; The State Council of China. The Outline of the Ecological Protection and High quality Development Plan of the Yellow River Basin. *Gaz. State Counc. People's Repub. China.* **2021**, *30*, 15–35.

56. The State Council of China. National Main Function Zone Plan. EB/OL. 2010. Available online: [http://www.gov.cn/zhengce/content/2011-06/08/content\\_1441.htm](http://www.gov.cn/zhengce/content/2011-06/08/content_1441.htm) (accessed on 7 November 2022).
57. National Development and Reform Commission; Ministry of Water Resources of the People's Republic of China; Ministry of Agriculture and Rural Affairs of the People's Republic of China; National Forestry and Grassland Administration. Outline of Comprehensive Management Plan for Loess Plateau Area (2010–2030). EB/OL. 2010. Available online: <https://zfxgk.ndrc.gov.cn/web/iteminfo.jsp?id=271> (accessed on 7 November 2022).
58. Ministry of Ecology and Environment of the People's Republic of China; Chinese Academy of Sciences. National Ecological Function Zoning (revised version). EB/OL. 2015. Available online: [https://www.mee.gov.cn/gkml/hbb/bgg/201511/t20151126\\_317777.htm](https://www.mee.gov.cn/gkml/hbb/bgg/201511/t20151126_317777.htm) (accessed on 7 November 2022).
59. Shang, J.; Cai, H.; Long, Y.; Zeng, J.; Chen, Y.; Zhang, X. Temporal-Spatial Distribution and Transition of Habitat Quality in Poyang Lake Region Based on InVEST Model. *Resour. Environ. Yangtze Basin* **2021**, *30*, 1901–1915.
60. Wang, J.; Yan, Y.; Wang, J.; Ying, L.; Tang, Q. Temporal-spatial variation characteristics and prediction of habitat quality in Min River Basin. *Acta Ecol. Sin.* **2021**, *41*, 5837–5848.
61. Gao, Q.; Pan, Y.; Liu, H. Spatial-temporal Evolution of Habitat Quality in the Dali Bai Autonomous Prefecture Based on the InVEST Model. *J. Ecol. Rural Environ.* **2021**, *37*, 402–408.
62. Wang, Y.; Gao, J.-X.; Jin, Y.; Cao, B.-S.; Wang, Y.; Zhang, X.-H.; Zhou, J.-W. Habitat Quality of Farming-Pastoral Ecotone in Bairin Right Banner, Inner Mongolia Based on Land Use Change and InVEST Model From 2005 to 2015. *J. Ecol. Rural Environ.* **2020**, *36*, 654–662. [[CrossRef](#)]
63. Xu, B.; Liu, Y.; Dong, Y.; Zhu, G.; Zhang, Y.; Lu, Z.; Zou, S. Evaluation of habitat quality in Lanzhou Region based on InVEST model. *J. Desert Res.* **2021**, *41*, 120–129.
64. Bao, Y.; Liu, K.; Li, T.; Hu, S. Effects of Land Use Change on Habitat Based on InVEST Model-Taking Yellow River Wetland Nature Reserve in Shaanxi Province as an Example. *Arid Zone Res.* **2015**, *32*, 622–629.
65. Zhao, X.; Shi, X.; Li, Y.; Li, Y.; Huang, P. Spatio-temporal pattern and functional zoning of ecosystem services in the karst mountainous areas of southeastern Yunnan. *Acta Geogr. Sin.* **2022**, *77*, 736–756.
66. Guo, Y.; Wang, N.; Chu, X.; Li, C.; Luo, X.; Feng, H. Analyzing vegetation coverage changes and its reasons on the Loess Plateau based on Google Earth Engine. *China Environ. Sci.* **2019**, *39*, 4804–4811.
67. Shenglin, M.; Zhouping, S. Characteristics and Causes of Land Use/Vegetation Coverage of the Loess Plateau in the Past 20 Years. *Res. Soil Water Conserv.* **2022**, *29*, 213–219. [[CrossRef](#)]
68. Naem, S.; Zhang, Y.; Zhang, X.; Tian, J.; Abbas, S.; Luo, L.; Meresa, H.K. Both climate and socioeconomic drivers contribute to vegetation greening of the Loess Plateau. *Sci. Bull.* **2021**, *66*, 1160–1163. [[CrossRef](#)]
69. Yang, J.; Xie, B.; Zhang, D. Spatial-temporal heterogeneity of ecosystem services trade-off synergy in the Yellow River Basin. *J. Desert Res.* **2021**, *41*, 78–87.
70. Song, Y.; Wang, M.; Sun, X.; Fan, Z. Quantitative assessment of the habitat quality dynamics in Yellow River Basin, China. *Environ. Monit. Assess.* **2021**, *193*, 614. [[CrossRef](#)] [[PubMed](#)]
71. Liu, C.; Yang, J.; Xie, B.; Chen, Y.; Pei, T. Temporal and spatial characteristics of habitat quality and its topographic gradient effect in the Gansu-Qinghai section of the Yellow River basin. *J. Agric. Resour. Environ.* **2020**, *1*–13. [[CrossRef](#)]
72. Liu, X.; Ren, Z.; Lin, Z.; Liu, Y.; Zhang, D. The spatial-temporal changes of vegetation coverage in the Three-River Headwater Region in recent 12 years. *Acta Geogr. Sin.* **2013**, *68*, 897–908.
73. Cheng-zhang, Z.; Liang-hong, J.I.A. Ecological performance and sustainable problems with the grazing forbidden project in the resource regions of the Yellow River. *J. Lanzhou Univ. Nat. Sci.* **2009**, *45*, 37–41.
74. Lei, Y. Trade-Offs and Collaborative Research on Major Ecosystem Services in San Jianguan Based on In VEST Model. Master's Thesis, Shanghai Normal University, Shanghai, China, 2020.
75. Lu, D.; Sun, D. Development and management tasks of the Yellow River Basin: A preliminary understanding and suggestion. *Acta Geogr. Sin.* **2019**, *74*, 2431–2436.